

1 **Reply to the editor's comment**

2  
3 Comment: I would encourage the authors to also consider how their work fits in with the evening  
4 transition top down process proposed by Caughey, S., & Kaimal, J. (1977). Vertical heat flux in  
5 the convective boundary layer. Quarterly Journal of the Royal Meteorological  
6 Society, 103(438).

7  
8 *Reply: Thank you very much for your suggestion. The above paper is very relevant to the*  
9 *present study and therefore those results are discussed in the discussion section.*

10 |  
11 **Replies to reviewer 1 comments**

12  
13 *At the outset we would like to thank the reviewer for his encouraging comments and useful*  
14 *suggestions.*

15  
16 The paper is based on boundary-layer measurements over a tropical rural site. The aim is to  
17 investigate afternoon-evening transition (AET). The authors present a detailed analysis of the  
18 phenomena on the basis of in-situ and remote sensing devices. The paper has certainly scientific  
19 interest to justify publication of these results. However, I have some concerns about the present  
20 version of the paper, and I believe that a careful revision of the paper is needed. I explain these  
21 issues in more detail below. I would encourage the authors to improve the English of the  
22 manuscript and re-submit.

23 *Reply: As per reviewers' suggestion, we tried our best to minimize the grammatical mistakes in*  
24 *the revised manuscript. Further, we have implemented all the suggestions given by the reviewer*  
25 *in the revised manuscript.*

26  
27 Specific Comments:

28  
29 Pag. 10, lines 1-2. To my knowledge, the water vapour mixing ratio ( $r$ ) and the specific humidity  
30 generally decrease at night due to vapour condensation. Is the strong increase of  $r$  measured at  
31 the surface around 14 IST typical of tropical sites?

32 *Reply: Yes. It is a typical phenomenon in the Tropics. It is mainly due to the continuous decrease*  
33 *of moisture transport into the mixed layer from the surface. Since most of the moisture sources*  
34 *are at the surface, the continuous waning of moisture transport by turbulence (thermals)*  
35 *increases the moisture at the surface. The vapor condensation does occur sometimes, but not*  
36 *during the evening transition. It generally occurs in the early morning during the winter period.*

37  
38 Figure 1e-h. The height coverage of the Sodar used by the authors is 0.03-1.5 km, but the  
39 maximum height where SNR is depicted is below 600-700 m also during the daytime, when  
40 strong convection is present up to 3 km (Figure 1i-l). Why?

41 *Reply: Although the maximum height for SODAR is fixed as 1.5 km, useful data comes from a*  
42 *height region of 30 m to ~600/800 m, depending on atmospheric conditions. Since the SODAR*  
43 *uses acoustic pulses, which generally gets attenuated quickly in the atmosphere, the height*  
44 *coverage is limited even in the presence of convection (during the day time).*

45 Pag. 10, line 8. Why does not the Sodar SNR signal show any increase at midday? The authors  
46 say that Figure 1e depicts an increase of SNR, but I do not see that increase.

1 *Reply: We agree that in the case presented here, the SNR enhancement is not significant. But it is*  
2 *clearly seen in many other cases. We, therefore, changed the text in the manuscript accordingly.*  
3 *However, the enhancement is clearly seen in Sodar spectral width and profiler SNR and spectral*  
4 *width images.*

5 Pag. 10, line 14. What do the authors mean with "horizontally stratified" ?

6 *Reply: What we mean by that statement is "The small-scale fluctuations in the SNR and spectral*  
7 *width primarily caused by the daytime turbulence are reduced during the nighttime. Both SNR*  
8 *and spectral width variations with time are small". To avoid confusion, we removed that part of*  
9 *the sentence and now the sentence read as "Nevertheless, about 2 h before the sunset, both the*  
10 *intensity and vertical extent of thermals start to decrease continuously till the sunset occurs."*  
11

12 Pag. 11, lines 11-12. The authors say that "Though the temperature decrement starts little early,  
13 but is not consistent and also weak in magnitude". In my opinion, Figure 2a shows a clear  
14 decrease of temperature starting from 1510 IST, with a rate of nearly 1°C per hour, which is of  
15 the same order of the rate used by the authors as one of the criteria to identify transition (0.5°C in  
16 30 min, see pag. 13). &

17 Pag. 11, lines 12-14. The mixing ratio grows suddenly also at nearly 1510 IST. It is not clear the  
18 criterion used by the authors to identify transition. Their choice seems to me somewhat arbitrary  
19 and questionable.

20 *Reply: We agree with the reviewer that the temperature decrement or mixing ratio increment*  
21 *starts at 1510 IST. But this decrement in 'T'/increment in 'r' is not consistent and the magnitude*  
22 *of decrement/increment is also small. As per our definition, the start time of evening transition is*  
23 *the time at which atmospheric state variables show large and persistent increase/decrease (i.e.,*  
24 *the increase/decrease should be significant and should persist for at least an hour). We*  
25 *examined the 19 cases, for which we have the data from all our instruments, and identified the*  
26 *start time of transition in each parameter manually. We then estimated the gradients in each*  
27 *parameter and finally fixed the thresholds based on these gradients. Later a sensitivity analysis*  
28 *is carried out to know the impact of the chosen thresholds on  $Trans_{sunset}$  as obtained by different*  
29 *state variables at different altitudes. We found that the results do not change much even if we*  
30 *vary each threshold by  $\pm 20\%$ . This new figure (shown for reviewers' reference) and the above*  
31 *information are included in the revised manuscript.*

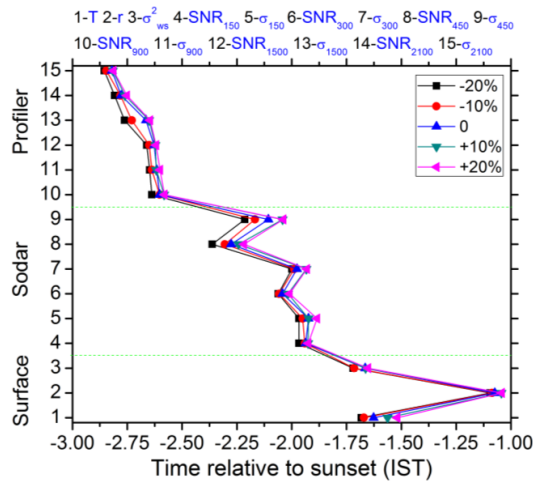


Figure:  $Trans_{sunset}$  identified by different instruments employing a variety of atmospheric state variables by varying the thresholds, indicating the sensitivity of  $Trans_{sunset}$  on the threshold.

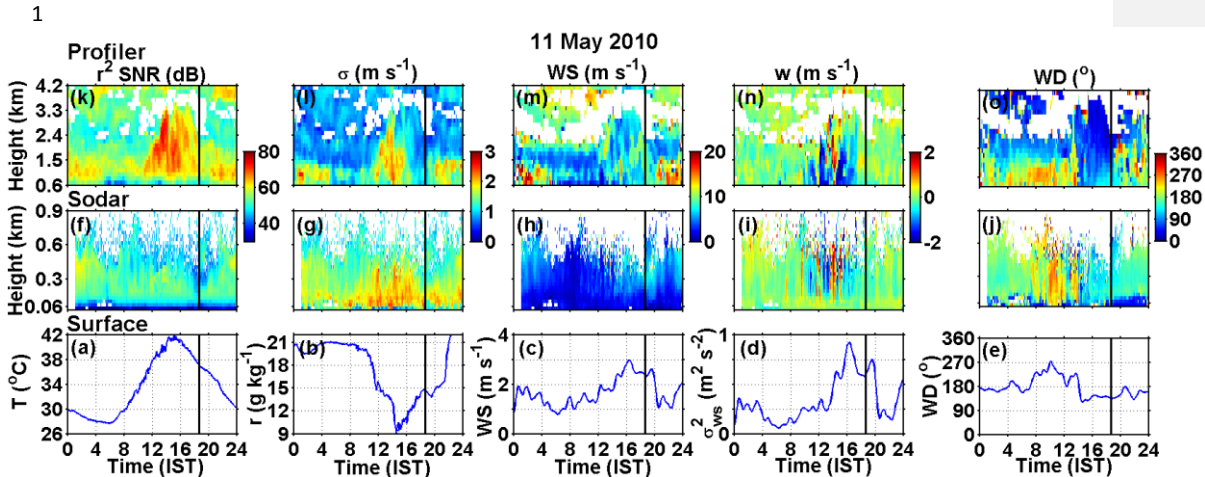
Pag. 11, lines 16-17. The time history of the wind variance is highly variable and shows several isolated peaks during the afternoon. Can the authors explain the reason why those peaks occur? I suggest to add the time history of the wind direction, it could help in identifying the passage of different air masses both near the surface and at elevated levels. Maybe, changes in  $r$  could be due to the different nature of such air masses. Furthermore, the vertical profile of wind direction might explain why the AET follows a top-to-bottom evolution.

&

Pag 14, lines 18-20. Again, I think the authors must add in their analysis the time history of the wind direction taken at several altitudes in order to check the possible presence of different air masses along the vertical, in particular during the AET.

*Reply: Since Gadanki is located in a complex terrain, sudden gusts will increase the wind variance. As correctly pointed out by the reviewer that it is difficult to identify the transitions from such noisy temporal variations. In fact, this is one of the reasons for not recommending variance as a parameter to identify the transition.*

*Yes. We agree with the reviewer that different air masses at different times or at different altitudes can cause gradients in the atmospheric state parameters or can give a clue to top-to-bottom evolution of transition. As suggested by the reviewer, time-height variation of wind direction is added to Figure 1. It clearly shows that the wind direction remained same (northeasterly) for about 3-4 hours during the transition, i.e., 2 hours before and after the sunset, at all heights below 1.5 km. It clearly indicates that the increase/decrease in atmospheric state variables is due to the evening transition rather than the passage of different air masses. Also, as we do not see any appreciable change in the wind direction at different altitudes before the sunset (it remained same at around  $130^\circ$ ), we can rule out the possibility of different air masses causing the top-to-bottom evolution of the evening transition. This information is included in the revised manuscript.*



2  
 3 **Figure: Time height variation of different atmospheric state variables on 11 May 2010, indicating**  
 4 **their diurnal variation.**

5 Pag 11, line 22. The SNR at  $z=450$  m decreases well before 16 IST. Furthermore, at  $z=300$  m  
 6 SNR is highly variable. I think that is not possible to give any definite conclusion based on the  
 7 sodar SNR.

8 *Reply: The variations in both SNR and spectral width during the daytime are primarily caused*  
 9 *by thermals. Though the strength of thermals continuously decrease during the transition, they*  
 10 *do cause enhancements in SNR and spectral width (see Figures 1l and 1g). As a result, we see*  
 11 *enhancements in SNR and spectral width (albeit small) overlaid on a general decreasing trend*  
 12 *during the transition. While choosing the thresholds, these complex variations are considered.*

13 Pag. 13, lines 1-7. Are the criteria listed by the authors appropriate only for tropical sites? In  
 14 other words, do they believe those criteria can be used in other contexts (non-tropical sites)?

15 *Reply: As mentioned above, some of the variations in state variables are typical of tropical sites.*  
 16 *Though other variables can be used at non-tropical sites, some tuning of the thresholds may be*  
 17 *required. This information is given in the revised manuscript.*

18 Pag. 19, line 11. The sensible heat flux is in the range  $0.15\text{-}0.25 \text{ Kms}^{-1}$ , and not  $1.5\text{-}2.5$ .

19 *Reply: Sorry for our mistake. It is now corrected in the revised manuscript.*

20 End of pag. 19 and beginning of pag. 20. The authors try to explain the top-to-bottom nature of  
 21 the AET on the basis of the values assumed by the entrainment ratio and the entrainment flux,  
 22 but, in my opinion, their explanation is not very convincing and, at the same time, is very  
 23 questionable. I would suggest to the authors to weaken their conclusions.

24 *Reply: The top-to-bottom evolution of the AET is very complex. In fact in the revised version, we*  
 25 *have added the advection term to the entrainment flux. Still the conclusions do not change much.*  
 26 *The present study clearly demonstrates that the AET follow the top-to-bottom evolution, and*  
 27 *gives an explanation for such an evolution. Keeping the complexity in the problem and*  
 28 *reviewers' suggestion in mind, we have diluted our conclusions on top-to-bottom evolution in the*  
 29 *revised manuscript.*

1 **Replies to reviewer 2 comments/suggestions**

2  
3 *At the outset we would like to thank the reviewer for his encouraging comments and useful*  
4 *suggestions.*

5  
6 The discussion paper presents a variety of observations of afternoon transitions. The  
7 observations are of good quality. Analysis at a tropical site adds something to the literature,  
8 which mostly has looked at mid-latitude situations. I think the paper could be a useful addition to  
9 the literature, but some aspects of the presentation need to be improved before publication.

10 *Reply: We thank the reviewer for his positive comments. We wish to inform that all suggestions*  
11 *given by the reviewer were considered and incorporated in the revised manuscript.*

12  
13 General comments:

14 1. The paper introduces a new term, "afternoon-evening transition." Transition terminology is  
15 already confusing enough. Please choose a term from the Lothon et al. paper.

16 *Reply: As per reviewers' suggestion, the afternoon evening transitions (AET) is modified as*  
17 *Afternoon Transition (AT) in the revised manuscript.*

18  
19 2. Since this is a tropical site, something should be said about how it is or should be different  
20 than a mid-latitude site. For example, does the smaller range of solar zenith angles matter to the  
21 range of transition times? What about the more rapid reduction of incoming radiation at lower  
22 latitudes?

23 *Reply: Yes...It, in deed, the incoming radiation differs at tropical and mid or high latitude sites,*  
24 *in terms of its magnitude, reduction during the afternoon, etc. All these factors impact the start*  
25 *time of transition, duration of transition, etc. A small note on this issue is included in the revised*  
26 *manuscript.*

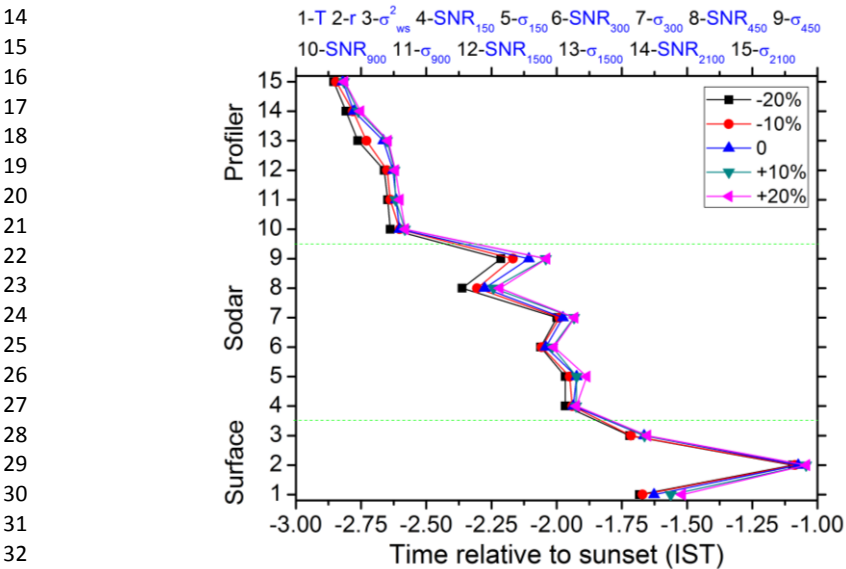
27  
28 3. By the time availability of data from all platforms is taken into account, the number of  
29 days included in each section of the study is small and different. Please be more clear about this,  
30 even to the point of being tedious and repetitive. A related point is that the filtering for clear-sky  
31 days must introduce important biases especially in the monsoon seasons. Again, this needs to be  
32 made very clear.

33 *Reply: As per reviewers' suggestion, the above information is included in Section 2 for each*  
34 *season, like total number of days in a season for which the instrument is operated and exclusion*  
35 *of data due to rain/dense clouds and quality. Since this information is given for each season, the*  
36 *biases, if any caused by the exclusion of data (say in monsoon season), will be known.*

	15m Tower (2009-2011)				Sodar (2007-2010)				Profiler ( 1999-00, 2010-11)			
Seasons	Win	Sum	SWM	NEM	Win	Sum	SWM	NEM	Win	Sum	SWM	NEM
Total no. of days	113	195	263	221	207	333	414	255	108	238	381	264
Discarded days	25	55	158	130	105	152	282	189	41	101	227	140
Clear days	88	140	105	91	102	181	132	66	67	137	154	124

1 4. The transition times are apparently chosen subjectively and are necessarily somewhat  
2 uncertain. This is not a problem, but should be made completely clear.

3 *Reply: The thresholds used in the present study are not chosen arbitrarily. As per our definition,*  
4 *the start time of evening transition is the time at which atmospheric state variables show large*  
5 *and consistent increase/decrease (i.e., the increase/decrease should be significant and should*  
6 *persist for at least an hour). We examined the 19 cases, for which we have the data from all our*  
7 *instruments, and identified the start time of transition in each parameter manually. We then*  
8 *estimated the gradients in each parameter and finally fixed the thresholds based on these*  
9 *gradients. Later, a sensitivity analysis is carried out to know the impact of the chosen thresholds*  
10 *on  $Trans_{sunset}$  as obtained by different state variables at different altitudes. We noticed that the*  
11 *results do not change much even if we vary the threshold by  $\pm 20\%$ . This new figure (included*  
12 *here for reviewers' reference) and the above information are included in the revised manuscript.*  
13



34 *Figure:  $Trans_{sunset}$  identified by different instruments employing a variety of atmospheric state*  
35 *variables by varying the thresholds, indicating the sensitivity of  $Trans_{sunset}$  on the threshold.*

36  
37 5. The word "collapse" should be removed everywhere it occurs, since the paper shows that it is  
38 an inappropriate way to think about the transition.

39 *Reply: Sorry. The word "collapse" is replaced with appropriate word (like 'fall', 'descend', etc.).*

40 6. The entrainment flux analysis starting on p.31498 is interesting but difficult. This has been  
41 attempted previously but with no success. The main difficulty in obtaining meaningful  
42 measurements of the very small mean vertical velocity. Advection, which is not included in eq.3  
43 but should be, is also usually important and very difficult to estimate. The results presented in  
44 figure 6 seem reasonable, but in order to give readers confidence that they are in fact correct,  
45 much more information is needed. A detailed uncertainty analysis should be done and error bars  
46 put on the fluxes. Some justification for the neglect of advection is also needed. If this harms the

1 flow of the paper too much, it could be put in an appendix or supplement, but it must be  
2 available to interested readers. Finally, figure 6 c and d are confusing because the days are run  
3 together as if they were continuous. At least the lines should be broken between the days, but a  
4 separate, larger figure might be better.

5 *Reply: We agree with the reviewer that the estimation and analysis of entrainment flux is*  
6 *difficult. Several authors earlier tried to estimate this flux (see Angevine (1999) and references*  
7 *therein). As per reviewers' suggestion, we have now added advection term to equation 3 and the*  
8 *figures are modified with complete entrainment flux (including advection term), error bars, and*  
9 *vertical dashed lines separating different days. In addition, the fluxes are shown in a separate*  
10 *figure as suggested by the reviewer.*

11  
12 7. A related point to the above is that, as shown here, the concept of entrainment ratio has limited  
13 applicability and should be used with caution.

14 *Reply: We do agree that the entrainment ratio, which is the ratio of entrainment and sensible*  
15 *heat fluxes, can vary due to the variation of any of those fluxes. The present study also shows the*  
16 *entrainment ratio variations are primarily caused (in our case) by sensible heat flux. Reviewers'*  
17 *suggestion is considered and the text is changed accordingly.*

18 8. In general the figures need to be bigger and more readable. Not all of this is under the direct  
19 control of authors, but I urge the authors to work with the journal staff to make readable figures.

20 *Reply: As per the reviewers' suggestion, we increased figures size, to depict the variations*  
21 *clearly. Also, figure 6 (in the old manuscript) is divided into two figures in the revised*  
22 *manuscript for clarity.*

23 Specific comments:

24  
25 1. Abstract, second paragraph: The wording is unclear. In fact the first evidence of the transition  
26 is aloft in the profiler data, followed by the sodar data and then the surface.

27 *Reply: We modified it in the revised manuscript.*

28 2. It seems that the SNR plots are not range-corrected. Is this true, and if so, why not? Plotting  
29 range-corrected SNR is clearer and more customary.

30 *Reply: Range corrected SNR plots are given in the revised manuscript.*

31 3. p.31495, top: Is there really not a consistent pattern between the radar and sodar? Elsewhere it  
32 is asserted that there is a significant difference in timing.

33 *Reply: What we mean here is that there is no consistent pattern in  $Trans_{sunset}$  as measured by*  
34 *SNR and spectral width at different altitudes (as measured by Sodar and Radar). For instance,*  
35 *SNR showing transition earlier than the spectral width or vice versa at a particular altitude.*  
36 *Nevertheless, there is a significant difference exists in the start time of transition as identified by*  
37 *Sodar and Radar. To avoid confusion, we modified the above sentence in the revised manuscript.*

38 4. p.31495 line 3 and p.31496 line 21: Why is it considered easier to use SNR than sigma? It  
39 looks to me like sigma is even clearer than SNR.

40 *Reply: In fact, the performance of SNR and sigma in identifying the transition is nearly the same*  
41 *and any one of them can be used for this purpose. The only reason we selected SNR is that it is*  
42 *consistent as evidenced by the narrow distribution of  $Trans_{sunset}$ . This point is made clear in the*  
43 *revised version of the manuscript.*

Formatted: Left



Replies to reviewer 3 comments

*At the outset we would like to thank the reviewer for his encouraging comments and useful suggestions.*

General Comments:

This paper give an interesting study of the afternoon to evening transitions (AET) over a tropical, rural site. Specifically, the paper seeks to answer three questions: (i) which state variable best identifies the onset of AET, (ii) does the onset of AET exhibit seasonal variability, (iii) does the onset of AET display height dependence? The researchers utilize an extensive, long term data set of both remote and in situ measurements throughout the entire ABL to address the questions. The researchers show that AET begins from the top-down and that there is some seasonal dependence due to high soil-moisture associated with the northeast monsoon. They assert that surface temperature and wind speed variance are the best signifier of the onset of AET at the surface and that the signal to noise ratio and spectral width are the best signifiers aloft. This is an interesting study and will be a welcomed addition to the literature. However, I do have several, general concerns that should be addressed before publication.

*Reply: We thank the reviewer for his positive comments. We wish to inform that all suggestions given by the reviewer were considered and incorporated in the revised manuscript.*

First, the thresholds for the onset of AET in each state variable (Pg 31493) seem somewhat arbitrary. For example, in Fig. 2a-b I feel one could also say that AET is beginning at the surface before it is aloft. This ambiguity may be inevitable but I feel that more explanation is merited. Perhaps a threshold sensitivity analysis could strengthen the authors' argument that the transition is top-down. Also, it'd be interesting to hear the authors hypothesize about any "universal" nature of the thresholds (i.e. would these apply at the mid-latitude sites).

&

31492 Ln 15: "On 11 May 2010, the temperature (Fig. 2a) starts to decrease monotonically, at the rate of 1–1.5 °C per 1 h, from 16:45 IST (dashed line), 118 min prior to the time of sunset (solid vertical black line). Though the temperature decrement starts little early, but is not consistent and also weak in magnitude". Again, I'm not sure I agree with this. To me, 16:10 looks more appropriate.

&

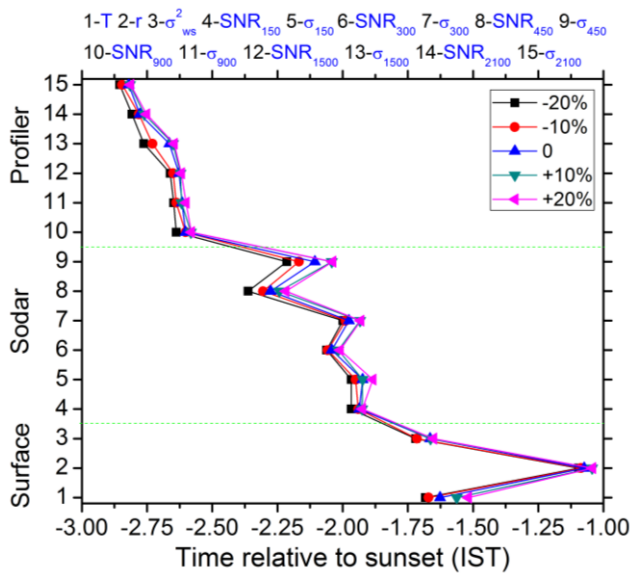
31492 Ln 16: "Another surface characteristic showing a significant change during the AET is the mixing ratio (Fig. 2b), which clearly shows a gradual increase from 16:10 IST". I do not think this is clearly shown.

*Reply: The thresholds used in the present study are not chosen arbitrarily. We agree with the reviewer that the temperature decrement or mixing ratio increment starts at 1510 IST. But this decrement in 'T'/increment in 'r' is not consistent and the magnitude of decrement/increment is also small. As per our definition, the start time of evening transition is the time at which atmospheric state variables shows large and consistent increase/decrease (i.e., the increase/decrease should be significant and should persist for at least an hour). We examined 19 cases, for which we have the data from all our instruments, and identified the start time of transition in each parameter manually. We then estimated the gradients in each parameter and finally fixed the thresholds based on these gradients. Later, a sensitivity analysis is carried out to know the impact of the chosen thresholds on  $Trans_{sunset}$  as obtained by different state variables at*



1 different altitudes. We noticed that the results do not change much even if we vary the threshold  
 2 by  $\pm 20\%$ . This new figure (shown below for reviewers' reference) and the above information are  
 3 included in the revised manuscript.

4  
 5 Some of the variations in state variables are typical of tropical sites. Though other variables can  
 6 be used at non-tropical sites, some tuning of the thresholds may be required. It is necessary,  
 7 because the solar zenith angle and the reduction of solar radiation are different at different  
 8 latitudes. Qualitatively, we can expect similar variations (either decrease or increase) in most of  
 9 the parameters at all latitudes, but the magnitude of variation could be different.



10  
 11  
 12  
 13  
 14  
 15  
 16  
 17  
 18  
 19  
 20  
 21  
 22  
 23  
 24  
 25  
 26  
 27  
 28  
 29  
 30  
 31 *Figure:  $Trans_{sunset}$  identified by different instruments employing a variety of atmospheric state  
 32 variables by varying the thresholds, indicating the sensitivity of  $Trans_{sunset}$  on the threshold.*

33  
 34 Second, the explanation given for the top-down behavior, specifically the ratio of the  
 35 entrainment to surface flux, is very interesting but also has a large degree of uncertainty. This  
 36 should be addressed in the paper.

37 *Reply: Yes. We agree with the reviewer that the entrainment flux estimation and its analysis is  
 38 very complex. In fact, we have added advection term to entrainment flux term for the sake of  
 39 completeness. But, still the results remain the same. As per reviewers' suggestion, the error in  
 40 the estimation of fluxes is added as an error bar. Also, an uncertainty analysis is included in the  
 41 revised manuscript.*

42  
 43 Third, some of the subfigures are too small to be easily studied.

44 *Reply: The size of figures is increased in the revised manuscript for better visualization.*

45 Finally, the overall readability and English of the paper could use some improvement.

46 *Reply: We tried our level best to remove the grammatical mistakes from the manuscript.*

1  
2  
3  
4  
5  
6  
7  
8  
9  
10  
11  
12  
13  
14  
15  
16  
17  
18  
19  
20  
21  
22  
23  
24  
25  
26  
27  
28  
29  
30  
31  
32  
33  
34  
35  
36  
37  
38  
39  
40  
41  
42  
43  
44

Specific Comments

31484 Ln 14-15: “The T at the surface and SNR aloft identify the signature of transition unambiguously”. Judging from Fig. 2, I disagree that it is unambiguous. Perhaps something like, “T at the surface and SNR aloft are the best indicators of transition”

*Reply: The sentence is modified in the revised manuscript.*

31488 Ln 17-24: I found the general description of the long-term and short-term data sets to be very confusing. Please re-word. Maybe something like, “dataset 1 was collected with a suite of non-continuously operated instruments, spanning a 3 year period. It is being used to examine AET seasonality and height dependence: : : Dataset 2 is comprised of the intensive observations which include the instrumentation of dataset 1 along with a flux tower and radiosondes launched every three hours. Dataset 2 was collected over two, three day campaigns (one during the monsoon and one during the winter).”

*Reply: In fact, the present study consists of 3 datasets and they are treated as dataset 1, dataset 2 and dataset 3 in the revised manuscript as per reviewers' suggestion.*

31489 Ln 24: Too bad the 50 m mast housed a single sonic at 8 m. It may or may not be worthwhile clarifying that in the Table 1 caption.

*Reply: The 50 m instrumented tower hosts both fast sensors (sonic anemometer-RM Young (81000) and infrared hygrometer-LI-COR) at two levels (4 m and 8 m) and slow sensors for meteorological parameters (temperature, relative humidity, wind speed and direction) at six levels (2, 4, 8, 16, 32 and 50 m). The pressure and shortwave radiation are measured at 1.2-m height. The shortwave radiation sensor, soil temperature and moisture profile probes and a tipping bucket rain gauge were installed 20 m away from the tower towards the south to minimize shadow effects. Details of the sensors and their temporal resolutions are given in Sandeep et al. (2014).*

*In Table 1, only the sensors used in the present study are given.*

31489 Ln 28-29: Please give a reference for the automated tests that were performed on the tower data. See comment 31499 Ln 22.

&

31499 Ln 22: “A stringent data quality check has been performed for the estimation of fluxes (Burba, 2013). These fluxes are evaluated at 30 min resolution.” This is more appropriate for section 2.

*Reply: The text discussing the data quality tests with reference is given in page no. 31499. As per reviewers' suggestion, the text is included here.*

31491 Ln 14: I'm not sure I see the increased backscatter in Fig. 1e.

*Reply: We agree that in the case presented here, the SNR enhancement is not significant. But it is clearly seen in many other cases. We, therefore, changed the text in the manuscript accordingly. However, the enhancement is clearly seen in Sodar spectral width and profiler SNR and spectral width images.*

1 31492 Ln 18: “The temperature gradient (Fig. 2c) also reverses from positive to negative,  
2 indicating the reversal of surface sensible heat flux, few minutes after the 5 m level 20  
3 temperature starts to decrease”. This isn’t necessarily the case. See “Countergradient heat flux  
4 observations during the evening transition period” (<http://www.atmoschem-phys.net/14/9077/2014/acp-14-9077-2014.html>).

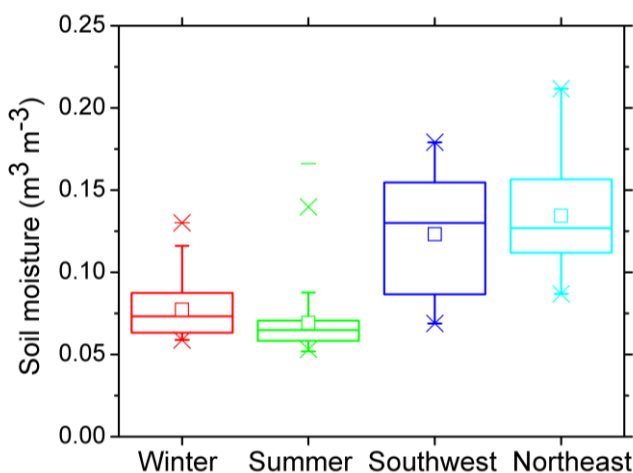
5  
6 *Reply: We modified the text by including this new reference and a note of caution.*

7  
8 31496 Ln 18-20: The questions the paper seeks to answer are given in the abstract, introduction,  
9 discussion and conclusion. Sometimes they are listed as 3 questions and sometimes as 4. While  
10 the general idea of the questions is approximately the same, it would help readability if they  
11 became more consistent.

12 *Reply: Sorry for that. In the revised version, we highlighted only 3 questions throughout the*  
13 *manuscript and tried to obtain answers for those questions.*

14  
15 31497 Ln 8: “Though Gadanki receives 55 % of the annual rainfall in the southwest monsoon,  
16 rising instantaneous soil moisture levels, but the high insolation and temperatures immediately  
17 consume the soil moisture for latent heating. On the other hand, this region also gets good  
18 amount of rainfall during the cool northeast monsoon (Rao et al., 2009). The soil moisture levels,  
19 therefore, remain high in this season.” Intuitively I agree with this. However, I’m wondering if  
20 there is any soil moisture data to help support it.

21 *Reply: Seasonal variation of soil moisture is shown below, as per reviewers’ suggestion, which*  
22 *clearly supports the text.*



23  
24 *Figure: Distribution of soil moisture in different seasons*

25  
26 31497 19: “It is known from the literature that there exists an apparent contradiction between  
27 those who think the transition starts in the afternoon at high levels (Angevine, 2008) and others  
28 who believe the AET occurs around the sunset and follows a bottom-up evolution. The present  
29 study supports the former view, as similar evolution is seen in total and seasonal plots (Figs. 3  
30 and 4).” Again, I’m not fully convinced that this isn’t at least partially due to the selected  
31 thresholds.

1 *Reply: We believe the top-to-bottom evolution in the afternoon transition is true as the present*  
2 *study clearly shows this evolution. Even if we assume that the chosen thresholds are not exact,*  
3 *the sensitivity analysis has clearly shown that the results do not change much even if we vary the*  
4 *thresholds by  $\pm 20\%$ . All the thresholds (within  $\pm 20\%$  of the chosen thresholds) show the top-to-*  
5 *bottom evolution of afternoon transition.*

6  
7 31500 Ln 4: “In contrast to large eddy simulations (LES) by Canut et al. (2012), who found an  
8 increase of the entrainment rate in the late afternoon, the present observations do not show any  
9 such increase, rather the entrainment flux remained constant throughout the day on all days”  
10 More discussion please. What are the weakness of the LES study vs yours?

11 *Reply: We included this sentence only to indicate that the entrainment flux can exhibit significant*  
12 *diurnal variation at some places, unlike at Gadanki. We believe too much discussion on the*  
13 *comparison of entrainment flux as obtained by LES and the present study and limitations and*  
14 *strengths in each method will certainly deviates the reader from the main topic. We, therefore,*  
15 *drop this sentence from the revised manuscript.*

16  
17  
18  
19  
20  
21  
22  
23  
24  
25  
26  
27  
28  
29  
30  
31  
32

1 | A comprehensive investigation on ~~Afternoon~~-afternoon ~~Evening Transition~~  
2 | transition of the atmospheric boundary layer over a tropical rural site  
3 |  
4 |

5 | A. Sandeep, T. Narayana Rao, and S.\_V.\_B. Rao#

6 | *National Atmospheric Research Laboratory, Gadanki – 517 112, India*

7 | *# Sri Venkateswara University, Department of Physics, Tirupati – 517 502, India*  
8 |  
9 |  
10 |  
11 |  
12 |

13 | Address for correspondence

14 | Dr. T. Narayana Rao

15 | Head, Clouds and Convective Systems Group

16 | National Atmospheric Research Laboratory

17 | Gadanki – 517 112, India

18 | Mail: [tnrao@narl.gov.in](mailto:tnrao@narl.gov.in)

19 | Alt. Mail [drtnr2001@yahoo.com](mailto:drtnr2001@yahoo.com)

20 | Phone: +91 8585 272 125  
21 |  
22 |  
23 |  
24 |  
25 |  
26 |

27 | **Keywords:** ~~Evening~~-Afternoon transition, Atmospheric boundary layer, Entrainment flux, sodar  
28 | and wind profilers.

1 | **Abstract:**

2 | The transitory nature of the atmospheric boundary layer few hours before and after the time of  
3 | sunset has been studied comprehensively over a tropical station, Gadanki (13.45°N, 79.18°E),  
4 | using a suite of in situ and remote sensing devices. This study addresses the following  
5 | fundamental and important issues related to the afternoon ~~to evening~~ transition (~~AET~~AT).  
6 | Which state variable first identifies it? Which variable best identifies it? Does the start time of  
7 | AET ~~varies~~ with season and height? If so, which physical mechanism is responsible for the  
8 | observed height variation in the start time of transition?

9 | At the surface, the transition is first seen in temperature ( $T$ ) and wind variance ( $\sigma^2_{ws}$ )~~at~~  
10 | ~~the surface~~, ~100 min prior to the time of sunset, then in vertical temperature gradient and finally  
11 | in water vapour mixing ratio variations. Aloft, both signal-to-noise ratio (SNR) and spectral  
12 | width ( $\sigma$ ) show the AT nearly at the same time. ~~the AET is observed nearly at the same time in~~  
13 | ~~signal to noise ratio (SNR) and spectral width ( $\sigma$ ) measurements of wind profiler and sodar.~~ The  
14 |  $T$  at the surface and SNR aloft ~~identify the signature of transition unambiguously~~ are found to be  
15 | the best indicators of transition. ~~Also,~~ ~~†~~ Their distributions for start time of AET with reference to  
16 | time of sunset are narrow and consistent in both total and seasonal plots. The start time of  
17 | transition shows some seasonal variation with delayed transitions occurring mostly in the rainy  
18 | and humid season of northeast monsoon. Interestingly, in contrast to the general perception, the  
19 | signature of the transition is first seen in the profiler data then in sodar data and finally in the  
20 | surface data, suggesting that the transition follows top-to-bottom evolution. It indicates that other  
21 | forcings, like entrainment, could also play a ~~major~~ role in altering the structure of ABL during  
22 | the AET, when the sensible heat flux decreases progressively. These forcing terms are

1 quantified using a unique high-resolution dataset to understand their variation in light of the  
2 intriguing height dependency of the start time of AET.

3

#### 4 **1. Introduction**

5 The behaviour of atmospheric boundary layer (ABL) during the transition from well mixed layer  
6 during the day to stably stratified layer during the night is quite complex and is also poorly  
7 understood. In recent years, the afternoon ~~to-evening~~-transition (AET) and evening transition  
8 (ET) of the ABL gained lot of attention for various reasons (Lothon et. al., 2014). These  
9 transitional regimes are found to be important for the vertical transport of species, like pollutants,  
10 water vapour and ozone (Klein et al., 2014), the inception and strength of the nocturnal low level  
11 jet (LLJ) (Mahrt, 1981; Van De Wiel et al., 2010), and the whole structure of the nocturnal  
12 boundary layer. Further, identification of ABL becomes uncertain and there is no consensus on  
13 which scaling laws (day-time convective scaling due to surface buoyancy flux? or nocturnal  
14 boundary layer scaling due to surface wind stress?) would work well during this period (Pino et  
15 al., 2006). Further, the start time of transition and its duration could be different at the surface  
16 and aloft, because the turbulence may not immediately dissipate after the sunset (Busse and  
17 Knupp, 2012).

18 Researchers defined the transition in a variety of ways employing various parameters  
19 obtained from different instruments. Some of them treated the transition as an instantaneous  
20 process, while the others considered it as a process of few hours. The most popular and widely  
21 used definition is the reversal of surface heat flux (positive to negative) (Grant, 1997; Acevedo  
22 and Fitzjarrald, 2001; Beare et al., 2006; Angevine, 2008). A similar technique is employed by  
23 Nieuwstadt and Brost (1986), in which the ~~AET~~AT is assumed to occur following the cessation



1 of upward surface sensible heat flux. Edwards et al. (2006) noted that the shortwave heating  
2 starts to decrease much before the surface heat flux changes its sign. They included the  
3 shortwave heating in the definition of AETAT, which shifted the start of afternoon transition to  
4 an earlier time. Acevedo and Fitzjarrald (2001) identified the start time of the transition from a  
5 sharp decrease in the spatial temperature difference and end from the maximum spatial standard  
6 deviation (~~SD~~) of temperature. As seen above, all these definitions are based on surface  
7 measurements and do not account the physical processes occurring aloft during the transition.

8 The studies that used remote sensing measurements like wind profiling radars, sodars and  
9 lidars focused more on the processes aloft (mostly in the lower part of ABL) to define the  
10 AETAT. In a seminal study, Mahrt (1981) used a kinematic definition for AETAT period.  
11 According to Mahrt (1981) the AETAT is a 4-5 h time period, starts from the time of low-level  
12 wind deceleration (typically 2 h before the sunset) and ends when the flow at all levels turned  
13 towards the high pressure. Grimsdell and Angevine (2002) and Angevine (2008), using radar  
14 wind profiler measurements, noticed that both reflectivity (range-corrected signal-to-noise-ratio  
15 (SNR)) and the spectral width ( $\sigma$ ) (a measure of turbulence) decrease sharply during the AETAT.  
16 The applicability of these approaches is always an issue, particularly when the turbulence is  
17 either weak or strong throughout the day or when the turbulence increases due to some other  
18 processes associated with katabatic winds or land see-breeze circulations (Sastre et al., 2012).  
19 Instead of defining the start and end times for AETAT, Busse and Knupp (2012) studied the  
20 variations in meteorological parameters with reference to the sunset time. They noted an increase  
21 in wind speed and a decrease in sodar return power in the lower ABL. They found that the  
22 AETAT has a relatively consistent pattern regardless of season.

1 A few studies employed models to understand or validate the occurrence of different  
2 types of transition (Brazel et al., 2005; Edwards et al., 2006; Pino et al., 2006; Sorbjan, 2007;  
3 Nadeau et al., 2011; Sastre et al., 2012). Brazel et al. (2005) studied the evening transition under  
4 weak synoptic forcing that favours the local thermal circulations and compared the observed  
5 transitions with models. Recently, Sastre et al. (2012) identified 3 types of evening transitions  
6 and evaluated performance of the Weather Research and Forecasting Advanced Research (WRF-  
7 ARW) model in reproducing these transitions by varying PBL parameterization schemes. They  
8 noted that all parameterizations reproduced the observed behaviour of AETAT in certain  
9 circumstances. Noting the need to understand the ~~evening~~ transitions in a better way, several  
10 field campaigns were conducted in recent years, employing both in situ and remote sensors,  
11 exclusively for better characterisation and modelling of the ~~evening~~ transitions. For instance,  
12 Cooperative Atmosphere-Surface Exchange Study (CASES-99) (Poulos et al., 2002), Boundary  
13 Layer Late Afternoon and Sunset Turbulence (BLLAST) (<http://bllast.sedoo.fr/>)(Lothon et al.,  
14 2014) and Phoenix Evening Transition Flow Experiment (TRANSFLEX) (Fernando et al.,  
15 2013). Recently, manned and unmanned aerial vehicles were used to study the vertical structure  
16 of lowest part of ABL during the AETAT (Bonin et al., 2013; Lothon et al., 2014).

17 Most of the above studies focussed on the variations in state variables, like temperature,  
18 humidity, wind and turbulence, in the surface layer as they are easily accessible. Other studies  
19 characterized the evening transitions aloft, but neglecting the variations at the surface. Only a  
20 few studies that were based on campaign data and/or a few months of data dealt the transitions in  
21 totality, i.e., studied the variations at the surface and aloft (Busse and Knupp, 2012; Fernando et  
22 al., 2013; Lothon et al., 2014). Again, the data employed in those studies were limited, few days  
23 to 2 months. Certainly there is a need to characterize and understand the transitions at the surface

1 and aloft in different seasons through systematic observations on a long-term basis. Further,  
2 earlier studies used different state variables to define the transition. Only a few studies focused  
3 on how these state variables vary with reference to the time of sunset (Busse and Knupp, 2012).  
4 Although some tower-based observations exist in the literature, the complete understanding of  
5 the transition over a deeper layer is certainly far from complete. This forms the basis for the  
6 present study. In particular, the study tries to ~~address~~ answer the following questions: ~~How~~ how  
7 the surface state variables and radar/sodar attributes vary during the transition and with reference  
8 to the time of sunset? Which state variable better identifies the transition? How the start time of  
9 transition varies with height and season? Which physical processes are responsible for the  
10 vertical evolution of the transition?

11 The paper is organized as follows: Sect. 2. introduces the measurement site, data and  
12 instrumentation employed. The variation of different state variables at the surface and aloft is  
13 studied with the help of a typical case study in Sect. 3. The start time of ~~AET~~ AT as identified by  
14 different state variables and their mean characteristics at the surface and aloft are studied with  
15 reference to the ~~start time of transition~~ time of sunset. The questions posed above are discussed  
16 in ~~the~~ light of present observations in Sect. 4. The important forcing terms on the ABL are  
17 estimated using a unique dataset to understand the role of entrainment in the ~~evening~~ afternoon  
18 transitions. The important results are concluded in Sect. 5.

## 20 **2: Data and ~~Site~~ site ~~Description~~ description:**

21 The present study follows an integrated approach, wherein several instruments available at  
22 National Atmospheric Research Laboratory (NARL), Gadanki (13.45° N, 79.18° E) are  
23 extensively used. This site is located ~375 m above the mean sea level in a rural area in southeast

1 peninsular India and is surrounded by hillocks (300-800 m within 10 km region) distributed in a  
2 complex fashion. The rainfall in this region is influenced primarily by two monsoons, southwest  
3 (June-September) and northeast (October-December) (Rao et al., 2009). Summer and winter are  
4 the other two seasons, covering the months of March-May and January-February, respectively.

5 The present study relies on a variety of instruments, both in situ and remote sensors  
6 (Table 1), whose measurements cover the entire ABL. Though these instruments provide several  
7 other parameters, those used in the present study are only listed in Table 1. Two kinds of  
8 datasets (~~we refer here~~ them here as dataset 1 and dataset 2) are used in the present study, but for  
9 different purposes. Dataset 1 was collected with a suite of non-continuously operated  
10 instruments, spanning a 3 year period. This dataset is being used to examine the seasonality and  
11 height dependence of AT. It includes ~~To study the vertical structure and the seasonality in AET,~~  
12 long-term observations made by an instrumented 15 m tower (hereafter referred to as Mini  
13 Boundary Layer Mast – MBLM), a Doppler sodar and three UHF wind profilers (operated at  
14 NARL, but during different years) ~~have been used~~. Dataset 2 is comprised of the intense  
15 observations, which include the instrumentation of dataset 1 along with a flux tower having a  
16 sonic anemometer (RM Young 8100) at 8 m level and radiosondes (Meisei 90) launched every  
17 three hours. Dataset 2 was collected over two, three day campaigns (one during the monsoon and  
18 one during the winter). ~~Whereas, few days of intense observations made by a flux tower and GPS~~  
19 ~~radiosonde (one ascent in 3 h) have been used to~~ This dataset is being used to understand the role  
20 of surface forcing and entrainment in triggering the ~~AET~~ AT.

21 The MBLM provides temperature ( $T$ ), relative humidity (RH), wind speed (WS) and  
22 wind direction (WD) data at 3 levels (5, 10 and 15 m) with 1 s temporal resolution. The type of  
23 sensors used and their accuracies are given in Table 2. A Doppler sodar operating at a frequency

1 of 1.8 kHz and a peak power of 100 W provides the SNR,  $\sigma$  and wind information at 27 s and 30  
2 m temporal and height resolutions, respectively (Anandan et al., 2008) (see Table 3 for more  
3 details about different remote sensing instruments). The UHF wind profiler data consists of the  
4 data from 3 wind profilers, operated during different years. An old UHF wind profiler (referred  
5 to as Lower Atmospheric Wind Profiler - LAWP) was operated at a frequency of 1.375 GHz  
6 during the period 1999-2000. Complete description of the system and specifications can be found  
7 in Reddy et al. (2001) and Rao et al. (2001). It was operated in two modes; low mode covering  
8 0.3 to 4.8 km and high mode covering 0.9 to 6.8 km, sequentially switching between each mode,  
9 providing a temporal resolution of  $\sim$ 11 min. Recently, NARL has indigenously developed two  
10 UHF wind profilers with the same frequency (1.28 GHz) but with different antenna dimensions  
11 and transmitted powers. The smaller UHF wind profiler that uses an 8 x 8 antenna array covering  
12 an area of 1.4 m x 1.4 m transmits a power of 0.8 kW (hereafter referred to as WPR<sub>8x8</sub>).  
13 Whereas, the larger profiler has a bigger antenna array of 2.8 m x 2.8 m with 16 x 16 elements  
14 and high-transmitting power of 1.2 kW (hereafter referred to as WPR<sub>16x16</sub>). Complete description  
15 of these systems and their capabilities can be found in Srinivasulu et al. (2011, 2012). The  
16 WPR<sub>8x8</sub> was operated at NARL during May-September 2010, while the bigger WPR<sub>16x16</sub> has  
17 been in operation from October 2010. It can be seen from Tables 1 and 3 that these instruments  
18 provide a unique long-term dataset from the surface to ~~the~~ top of the ABL.

19 ~~These long term measurements are augmented by intense observations made in a~~  
20 ~~campaign, wherein GPS radiosondes (Meisei 90) have been launched for every 3 h for 3~~  
21 ~~successive days. Also a 50 m micrometeorological flux tower housing a sonic anemometer (RM~~  
22 ~~Young 8100) at 8 m level (with 20 Hz temporal resolution) is also employed for the estimation~~

1 ~~of sensible heat flux. Two such campaigns were conducted, one each in southwest monsoon and~~  
2 ~~winter.~~

3 A series of automated tests were performed on tower time series data to identify  
4 instrumentation problems, flux sampling problems, and physically plausible but unusual  
5 situations (Burba, 2013). Further, clear-sky days are identified from shortwave radiation  
6 measurements made by a pyranometer (Kipp and Zonen CMP6) located near the MBLM.  
7 Omitting the days with large data gaps and rain/dense clouds, 423 days of surface data were  
8 available for further analysis from 3 years of MBLM measurements. The range-time plots of  
9 spectral moments (SNR, vertical velocity ( $w$ ) and  $\sigma$ ) from sodar and wind profiler are examined  
10 for the clear growth and decay of ABL and convection/precipitation contamination (Grimsdell et  
11 al., 2002; Rao et al., 2008). Based on the above criteria, a total of 530 and 482 clear-sky days of  
12 sodar and ~~radar~~ profiler, respectively, were only selected (from dataset 1) for further analysis. To  
13 examine whether the filtering of data for clear-sky days has caused any bias towards the dry  
14 season (winter and summer), the data are segregated on the basis of season. Table 4 shows the  
15 number of days for which the measurements were available, ~~excluded~~ number of discarded days  
16 due to rain/dense cloud or bad data ~~gap~~ quality and the number of days considered for the present  
17 study as a function of season. Though considerable data were filtered out in the rainy seasons  
18 (southwest and northeast monsoons), the number of available days is large enough to represent  
19 the season. Also, the number of days available in the rainy season is of the same order as that of  
20 in other seasons, indicating that the filtering has not biased the results towards any season.

21 Note that MBLM, sodar and wind profilers were operated during different years. Only 19  
22 days of simultaneous clear-sky measurements (without large data gaps) from all the above  
23 sensors were available. Measurements from these 19 days are used to understand the behavior of

1 ~~AETAT~~ at different altitudes. The total data (from different years, i.e., dataset 1) are used to  
2 obtain robust statistics on the mean behavior of ~~AETAT~~.

### 3 **3. Results and ~~Discussion~~discussion:**

#### 4 **3.1. Typical evolution of ~~AETAT~~ from the surface to ~~the top of the ABL~~:**

5 Figure 1 shows the diurnal variation of surface state variables ( $T$ , water vapour mixing ratio ( $r$ ),  
6 ~~WS~~, ~~and~~ wind variance ( $\sigma^2_{ws}$ ) and wind direction (WD)) and sodar and profiler attributes (range-  
7 corrected SNR (hereafter referred to simply as SNR), horizontal wind speed,  $\sigma$ , ~~and~~ w and wind  
8 direction) on 11 May 2010, providing a comprehensive paradigm of the typical evolution of ~~the~~  
9 ~~evening~~ transitional boundary layer at the surface and aloft (up to 3.6 km). The surface state  
10 variables (at 5 m level) exhibit larger variations during the transition period than during rest of  
11 the night. During the ~~AETAT~~, as the shortwave heating decreases, the temperature decreases  
12 monotonically (Fig. 1a) in clear-sky conditions, if temperature advection is neutral. Another  
13 signature of this transition can be seen in short-term variability of surface parameters, highly  
14 variable during the noon (associated with thermals) to smaller fluctuations in the night. The  
15 weakening of thermals (both magnitude and their vertical extent) in the afternoon reduces the  
16 convective turbulence and  $\sigma^2_{ws}$  (Fig. 1d). This reduction weakens the downward transport of  
17 momentum and low-level wind speed (Fig. 1c) (Mahrt, 1981; Acevedo and Fitzjarrald, 2001).  
18 The surface winds also became less gusty during the transition. During the day, when the  
19 convective turbulence is active, the low-level moisture gets diluted because of the transport of  
20 moisture by turbulence. As the turbulence decreases during the transition, the low-level moisture  
21 having most of its sources on the earth's surface increases in the absence of strong mixing (Fig.  
22 1b). On some days, this increase appears as a sudden jump, as also noted by earlier studies  
23 (Busse and Knupp, 2012), and on the other days it is more gradual. The wind direction nearly



1 | remains the same from ~14 IST (Indian Standard Time (IST) = UTC + 05:30) to mid-night (Fig.  
2 | 1e).

3 | To understand the transitions aloft, variation of sodar and profiler attributes are examined  
4 | in detail (~~Figures Fig. 1f-e-l~~o). Figure 1 clearly shows the transition of the ABL from a highly  
5 | convective to a more stable regime. When the convective turbulence is active during the day  
6 | time, the thermals are clearly apparent as columns of enhanced backscatter in the time-height  
7 | SNR plot (Fig. ~~1k&-h~~). Though the thermals do not appear clearly in the SNR of sodar in this  
8 | case, they appear very clearly in other cases. These plumes are also visible in the  $w$  plot (Fig. ~~h~~  
9 | ~~l~~i and ~~h~~n) as enhanced up- and down-ward motions with  $w$  values exceeding  $\pm 2 \text{ m s}^{-1}$  and as  
10 | columns of enhanced turbulence (Fig. ~~1g~~ and ~~h~~j). The backscatter for sodar and ~~radar profiler~~  
11 | depends on the refractive index irregularities caused primarily by turbulence-driven temperature  
12 | and humidity variations. The SNR is, therefore, high during the day, when the convectively-  
13 | driven turbulence is active. Nevertheless, about 2 h before the sunset, both the intensity and  
14 | vertical extent of thermals start to decrease continuously till the sunset occurs,~~with time before~~  
15 | ~~they became horizontally stratified.~~ The minimum backscatter (SNR) is seen just before the  
16 | sunset, mainly due to the weak turbulence. The magnitude of backscatter and ~~the~~-vertical extent  
17 | of sodar data again increase in accordance with the deepening of the inversion layer. As noted by  
18 | Busse and Knupp (2012), the winds within the nocturnal boundary layer generally decrease  
19 | during the ~~AETAT~~, but increase above the nocturnal boundary layer. It makes the identification  
20 | of start time of ~~AETAT~~ using wind speed somewhat ambiguous. On the other hand, it is rather  
21 | easy to identify the start time of ~~AETAT~~ from the variations of SNR and  $\sigma$ . The wind direction  
22 | does not change much with altitude below 1.5 km and remains mostly easterly to southeasterly  
23 | (Figures. 1j and 1o). It doesn't change much with time also around the time of sunset (few hours

1 before and after the time of sunset), ruling out the possibility of advection of ~~a~~-different air  
2 masses causing the above changes.

3       When the surface heating reverses to cooling in the evening, both convection and  
4 turbulence gradually reduces till the subsequent development of a stable boundary layer with  
5 well-defined surface inversion layer. As a result, all state variables at the surface and aloft,  
6 manifested primarily by the turbulence, vary considerably during this period. To better depict  
7 this variability, MBLM- ( $T$ ,  $r$ ,  $\sigma_{ws}^2$  and  $\Delta T$  ( $T_5-T_{10}$ , indicating the stability of the lower ABL, the  
8 suffixes 5 and 10 indicate the height of temperature measurements in m)), sodar- and profiler-  
9 derived state variables (SNR and  $\sigma$  at 3 representative levels; 150, 300 and 450 m for sodar and  
10 900, 1500 and 2100 m for ~~radar~~profiler) during the period 15:00–21:00 IST (~~Indian Standard~~  
11 ~~Time (IST) = UTC + 05:30~~) are plotted in Fig. 2. To minimize random fluctuations and the  
12 chosen level more representative, the data are averaged both in time (5 min for sodar and no  
13 temporal integration for ~~radar~~profiler) and height (3 heights centred on the chosen level). The  
14 time series surface data are then low-pass filtered using local regression using weighted linear  
15 least squares and a 1<sup>st</sup> order polynomial model (using the function ‘lowess’ in matlab). On 11  
16 May 2010, the temperature (Fig. 2a) starts to decrease monotonically, at the rate of 1-1.5 °C per  
17 1 h, from 16:10~~45~~ IST (dashed line), ~~118-152~~ min prior to the time of sunset (solid vertical black  
18 line). Though the temperature decrement starts little early, but is not consistent and also weak in  
19 magnitude. Another surface characteristic showing a significant change during the ~~AETAT~~ is the  
20 mixing ratio (Fig. 2b), which clearly shows a gradual increase from 16:10 IST. The temperature  
21 gradient (Fig. 2c) also reverses from positive to negative, ~~indicating the reversal of surface~~  
22 ~~sensible heat flux~~, few minutes after the 5 m level temperature starts to decrease. The wind

1 variance (Fig. 2d), representing small-scale wind fluctuations and turbulence, also shows a  
2 decreasing trend from 16:45-25 IST.

3 The sodar and profiler backscatter, depends primarily on turbulent irregularities of  
4 refractive index, decreases with the waning of sensible heat flux (and thermals) during the  
5 afternoon transition. On 11 May 2010, the SNR of sodar starts to decrease ~2 h 40 min prior to  
6 the time of sunset at all heights. Interestingly, the start time of SNR reduction shows height  
7 dependence with higher altitudes showing the reduction earlier. The SNR minimum is observed  
8 10-20 min before the sunset at all heights, mainly due to the reduction in turbulent fluctuations in  
9 temperature. Nevertheless, the SNR increases again after the sunset, following the formation of  
10 an inversion layer. The  $\sigma$  (Fig. 2f) variations are quite similar to that of SNR during the  
11 transition. The  $\sigma$  shows a decreasing trend 2 h 10-20 min prior to the sunset, whereas its  
12 minimum is observed 10-30 min from the time of sunset. The profiler SNR and  $\sigma$  variations are  
13 similar to that of sodar, except that their reduction starts little early. The profiler SNR and  $\sigma$  start  
14 to decrease ~3 h prior to the time of sunset. Also, the SNR and  $\sigma$  minima are observed at around  
15 the time of sunset. It is very interesting to note the height dependency in the time at which state  
16 variables show large variation, i.e., it is seen first in profiler attributes then in sodar attributes and  
17 finally in surface parameters.

### 18 **3.2. Distributions for start time of transition with reference to the time of sunset:**

19 It is clear from the case study that surface parameters and sodar/profiler attributes show large  
20 variations during the AETAT. The first and foremost problem, therefore, is to properly and  
21 objectively identify the start time of AETAT from these state variables. It is also important to  
22 recognize the state variable that unambiguously identifies the start time of transition. As seen in  
23 case studies, state variables like  $T$ ,  $\Delta T$ ,  $r$  and  $\sigma_{WS}^2$  at the surface and SNR and  $\sigma$  aloft can be used

1 | for this purpose. For identifying the start time of AETAT, 19 days on which measurements of all  
2 | instruments (MBLM, sodar and profiler) are available are considered. The start time of AETAT  
3 | is identified manually from temporal variation of each state variable (like those shown in Fig. 2).  
4 | The temporal gradients are estimated for each state variable from all 19 cases, which are then  
5 | finally used to fix the thresholds. The start time of AETAT is identified from the variation of the  
6 | each state variable as follows.

7 | Temperature: the time at which  $T$  starts to decrease by  $\geq 0.5^\circ\text{C}$  in 30 min.

8 | Water vapour mixing ratio: the time at which  $r$  increases by  $\geq 0.5 \text{ g kg}^{-1}$  in 30 min.

9 | Wind variance: the time at which  $\sigma_{ws}^2$  decreases by  $\geq 0.1 \text{ m}^2 \text{ s}^{-2}$  in 30 min.

10 | Temperature gradient: the time at which  $\Delta T$  becomes positive to negative and remains negative  
11 | for at least an hour.

12 | SNR: the time at which SNR decreases by  $>_1 \text{ dB}$  in 30 min.

13 | Spectral width: the time at which ~~the~~  $\sigma$  decreases by  $\geq 0.1 \text{ m s}^{-1}$  in 30 min.

14 | Note that all the above conditions should hold good for at least an hour from the start time of  
15 | transition. Also, all the above conditions are checked only in the data during 15:00-20:00 IST.

16 | First, the average behaviour of the start time of AETAT, as identified by selected state  
17 | variables, with reference to the sunset (i.e., start time of AETAT – time of sunset) has been  
18 | studied at the surface and aloft. The distributions (from ~~whole dataset~~ dataset 1) for start time of  
19 | AETAT with reference to the sunset (hereafter referred to as  $\text{Trans}_{\text{sunset}}$  (start time of AETAT –  
20 | time of sunset)) as obtained by various state variables are shown in Fig. 3. These distributions are  
21 | shown as box plots, where the box comprises 50 % of values (25 and 75 percentile) and whiskers  
22 | represent 5 and 95 % percentile values. On average,  $\sigma_{ws}^2$  and  $T$  show the first signature of  
23 | AETAT among all surface state variables (Fig. 3a),  $\sim 1 \text{ h } 40 \text{ min}$  prior to the time of sunset,

1 | followed by  $\Delta T$  (1 h 18 min before sunset). The last characteristic for ~~the~~ transition is seen in  $r$  as  
2 | a gradual increase (or jump) occurring, 1 h 10 min prior to the time of sunset. The signature of  
3 | transition can be seen as early (late) as 165 (45) min before (after) the sunset in ~~wind-variance~~  
4 |  $\sigma_{ws}^2(r)$  on some days. Except for temperature, all other surface state variables show signature of  
5 | transition even after the sunset. Though not many such cases are found at Gadanki (can be seen  
6 | from Fig. 3a), but late ~~evening~~ transitions are not uncommon, as they are widely reported  
7 | elsewhere (Acevedo and Fitzjarrald, 2001). The distribution of  $\text{Trans}_{\text{sunset}}$  is wider for  $r$  than for  
8 | any other state variable, indicating that the jump in  $r$  occurs at different timings with reference to  
9 | the time of sunset. On the other hand, the start time of ~~AET~~AT as obtained by  $T$  is relatively  
10 | consistent throughout the year, as evidenced by the narrow distribution (Fig. 3a).

11 | Figure 3b-~~3~~g shows distributions for  $\text{Trans}_{\text{sunset}}$  as identified by selected sodar and profiler  
12 | attributes (SNR and  $\sigma$ ) at 3 selected altitudes (150, 300 and 450 m for sodar and 900, 1500 and  
13 | 2100 m for ~~radar~~ profiler). At any particular altitude, ~~On average,~~ both SNR and  $\sigma$  shows the  
14 | signature of transition around the same time. Though small differences exist, they are not  
15 | significant ~~and do not show any consistent pattern with altitude or between the radar and sodar.~~  
16 | Nevertheless, the identification of transition start time is somewhat easy with SNR and is also  
17 | consistent, as evidenced by its relatively narrow distribution.

18 | As seen in the case study, the mean start time of ~~AET~~AT also shows height dependency  
19 | and follows top-to-bottom evolution, i.e., the signature of ~~AET~~AT is seen first in the profiler data  
20 | (~2 h 40 min before the time of sunset) then in sodar data (~2 h before the time of sunset) and  
21 | finally in MBLM measurements. Angevine (2008) also noted the deterioration of ABL structure  
22 | aloft with wind profiler preceding the start time of ~~AET~~AT at the surface. It contradicts the  
23 | general perception that the entire ABL is controlled primarily by the underlying earth's surface

1 and the start time of transition should follow a bottom-up evolution. It is true that surface forcing  
2 is the defining mechanism during the day, but it seems not the case during the transition, the time  
3 during which other forces could also be important.

4 A sensitivity analysis is carried out to know the impact of the above chosen thresholds on  
5 Trans<sub>sunset</sub> as obtained by different state variables. The chosen thresholds are varied by ± 20-% in  
6 steps of 10-% and the mean Trans<sub>sunset</sub> as obtained by different state variables is estimated at  
7 different altitudes. The mean Trans<sub>sunset</sub> as a function of altitude is plotted in Fig. 4, which clearly  
8 shows that the important results do not change much, even if we vary the thresholds by ± 20-%.  
9 For instance, the mean Trans<sub>sunset</sub> does not change much with the variation of thresholds. Also,  
10 the height dependence of Trans<sub>sunset</sub> is strikingly apparent with all used thresholds. It suggests  
11 that the observed variability in Trans<sub>sunset</sub>, like top-to-bottom evolution, is not an artefact arising  
12 due to the chosen thresholds. Regarding the usability of these thresholds at other sites, it appears  
13 (from Fig. 4) that they possibly can be used at other tropical sites, which are in similar climatic  
14 conditions as Gadanki region. Although we expect similar variations in most of the state  
15 parameters at mid- and high-latitudes, the magnitude of variation could be different because of  
16 the differences in the solar zenith angle and rate of reduction of solar radiation during the  
17 transition. Therefore, some tuning of thresholds may be required at different latitudes.

Formatted: Subscript

### 19 **3.3. Seasonal variation in the start time of transition:**

20 Since Gadanki experiences different seasonal patterns: very hot and dry summer, hot and rainy  
21 southwest monsoon, cool and rainy northeast monsoon and cool and dry winter. These seasonal  
22 factors (solar exposure, synoptic flow, soil condition, etc.) will have a different impact on ABL,  
23 in general, transitions, in particular. Therefore, the distributions of Trans<sub>sunset</sub> for different

1 seasons (Fig. 45) have been studied to understand the impact of the above factors on the start  
2 time of transition. Figure 4a5a-4d-d reveals that the order in which the surface state variables  
3 show the transition remain nearly the same (monsoon season is an exception), but their  
4 occurrence time with reference to the sunset varies considerably. Although reduced compared to  
5 the total data (Fig. 3), the distribution, representing the variability within the season, of transition  
6 start time for each state variable is quite wide. The  $\text{Trans}_{\text{sunset}}$  distribution for  $T$  shows a  
7 consistent pattern regardless of season with small variability within the season and the transition  
8 starts 80-100 min prior to the time of sunset. Nevertheless, it exhibits a clear seasonal variation  
9 with dry seasons (winter and summer) showing the transition early (~110 min prior to the sunset  
10 time) compared to rainy seasons (80 min prior to the sunset time). The distributions for other  
11 state variables also show some seasonal variation with warm seasons showing the transition little  
12 earlier than cold seasons. But their distributions are much wider than the observed weak seasonal  
13 variation. Among all state variables,  $\text{Trans}_{\text{sunset}}$  distribution for  $r$  shows not only large seasonal  
14 variability but also a wide distribution, indicating highly variable nature of  $r$  jump (i.e., starts at  
15 different timings with reference to the sunset).

16 Two representative heights, 300 m from sodar and 1500 m from wind profiler, are chosen  
17 to study the seasonal variation in transition start time aloft (Fig. 4e5e-51). Like in Fig. 3, there is  
18 not much difference in the start time of transition by SNR and  $\sigma$  in any season and at any  
19 particular altitude. Two observations are strikingly apparent from Fig. 45. 1. Both profiler- and  
20 sodar-derived start time of transition shows some seasonal variation with delayed transition  
21 during the northeast monsoon, consistent with the seasonal variation at the surface. 2.  
22 Irrespective of the season, the height dependency in transition start time is intact. Both these  
23 issues are discussed in detail in Sect. 4.



#### 1 | ~~4.~~ Discussion:

2 | The ~~four~~three major questions related to the start time of transition that the paper tries to answer  
3 | are, (i) which state variable better identifies it, (ii) does it exhibits any seasonal variation ~~and~~ (iii)  
4 | does it shows any height dependency?, and (iv) which physical mechanism is responsible for the  
5 | observed height variation of  $Trans_{sunset}$ ?

6 | (i) Among all state variables, the decrease of temperature at the surface and SNR aloft are  
7 | strikingly apparent in all case studies, which makes them ideal to identify the start time of  
8 | ~~AETAT~~. Further, the distributions of  $Trans_{sunset}$  for  $T$  and SNR are somewhat consistent and  
9 | narrower than that for other state variables. Although several earlier studies employed reversal of  
10 | sign in surface heat flux as a criterion for transition (Lothon et al., 2014 and references therein),  
11 | it is now well known that such a reversal not always occurs during the transition (Busse and  
12 | Knupp, 2012). The formation of an inversion depends on several other factors and therefore the  
13 | formation of inversion alone cannot be used to define the transition. A few studies used  
14 | deceleration of low-level wind as a criterion for identifying the transition (Mahrt, 1981). The  
15 | above criterion works well in the lower portion of ABL, but fails above the nocturnal boundary  
16 | layer, where the wind accelerates in the frictionless fluid. Therefore,  $T$  at the surface and SNR  
17 | aloft can be used to identify the start ~~of~~ time of transition ~~unambiguously~~, as also suggested by  
18 | Edwards et al. (2006).

19 | (ii) The start time of transition as defined by different state variables shows some seasonal  
20 | variation, with late transitions during the northeast monsoon season. Though Gadanki receives  
21 | 55-% of the annual rainfall in the southwest monsoon, rising instantaneous soil moisture levels,  
22 | but the high insolation and temperatures immediately consume the soil moisture for latent  
23 | heating. On the other hand, this region also gets good amount of rainfall during the cool

1 northeast monsoon (Rao et al., 2009). The soil moisture levels, therefore, remain high in this  
2 season. It is known from earlier studies that the abundance of soil moisture not only produces  
3 shallow ABL but also delays the growth of the ABL (Sandeep et al., 2014). It appears from  
4 present observations that not only the growth but also the ~~collapse~~descend (or transition) is  
5 getting delayed due to the excess soil moisture.

6 (iii) The total and seasonal distributions of  $Trans_{\text{sunset}}$  for different state variables at the surface  
7 and aloft clearly show the height dependency in the start time of transition, following a top-to-  
8 bottom evolution. It is known from the literature that there exists an apparent contradiction  
9 between those who think the transition starts in the afternoon at high levels (Angevine, 2008) and  
10 others who believe the AETAT occurs around the sunset and follows a bottom-up evolution. The  
11 present study supports the former view, as similar evolution is seen in total and seasonal plots  
12 (Figs. 3 and 45). During the AETAT, when the surface buoyancy flux decreases toward zero, the  
13 influence of other competing processes like advection, and entrainment becomes relatively more  
14 important (Bosveld et al., 2014). Therefore an attempt has been made to estimate these fluxes  
15 (buoyancy and entrainment) to understand their roles in the observed height dependency in  
16 transition start time.

17 The ratio between the vertical kinematic eddy heat flux at the top of ABL and kinematic  
18 eddy heat flux at the surface (entrainment ratio) (Sun et al., 2008), as given below, therefore,  
19 becomes a fundamental and decisive parameter.

$$20 \quad A_{*R} = -\frac{\overline{(w|\theta|)}_{z_t}}{\overline{(w|\theta|)}_s} \quad \dots (1)$$

21 The heat flux at the top of ABL (or entrainment flux) is estimated following Angevine (1999).

22 The entrainment can occur due to any or all of these factors, (1) when there is a shift in the ABL

1 height (2) due to wind shear at the ~~top of the ABL surface, and~~ (3) due to wind shear at the  
 2 ~~surface~~ top of the ABL and (4) advection.

$$3 \quad -(\overline{w|\theta|})_{zi} = A_0 + (A_2 u_*^2 u + A_3 \Delta u_h^3) (\theta_{vo}/gd_l) \pm (U \frac{\partial T}{\partial x} + V \frac{\partial T}{\partial y}) \dots (2)$$

4 where  $u_*$  is the friction velocity,  $u$  the surface horizontal velocity (5-8 m in our case),  $\Delta u_h$  the  
 5 wind shear at the top of ABL,  $g$  the acceleration due to gravity,  $\theta_{vo}$  the virtual potential  
 6 temperature at the surface,  $d_l$  is the depth of entrainment zone and  $A_2$  and  $A_3$  are empirical  
 7 constants,  $A_2=0.005$  and  $A_3=0.01$  (Stull, 1976). For the estimation of advection (last term in Eq.  
 8 2), the temperature ( $T$ ), horizontal distance in zonal and meridional planes ( $\partial x$  and  $\partial y$ ,  
 9 respectively, and is equal to  $0.5^\circ$ ) and zonal ( $U$ ) and meridional ( $V$ ) wind velocities ~~at~~ near the top  
 10 of ABL are taken from ECMWF Interim Reanalysis data (Dee et al., 2011).  $A_0$  is the entrainment  
 11 flux in the absence of any mechanical term contribution and is expressed as  $w_e \Delta \theta$ ,  $w_e$  is the  
 12 entrainment velocity and is estimated as follows.

$$13 \quad w_e = \frac{dz_i}{dt} - \bar{w} \dots (3)$$

14 where  $\bar{w}$  is the average vertical velocity at the top of ABL and  $\Delta \theta$  the vertical gradient in  $\theta$ , at  
 15 the top of ABL. As seen above, the time and space scales of different entrainment processes  
 16 cover a wide range, which makes it difficult to measure or model accurately (Angevine 1999).  
 17 Although it is possible to quantify the entrainment flux from heat budget equation (Eq. 2), the  
 18 uncertainties in the basic parameters (for instance, those in the advection term and  $w$ ) hamper the  
 19 accuracy of the flux. Therefore, as also pointed by Angevine (1999), these numbers need to be  
 20 considered as 'best available estimates'.

21 It is clear from above equations that profiles of meteorological parameters such as  $T$ ,  
 22 RH/ $r$  and  $w$  are essential to estimate the entrainment ratio. Though  $w$  can be obtained  
 23 continuously from the wind profiler, continuous measurement of  $T$  and RH/ $r$  at the top of ABL is

1 a difficult task. We, therefore, considered two 3 days campaign data (one each from southwest  
2 monsoon and winter), wherein radiosonde ascents were made once in  $\sim 3$  h, for a detailed study  
3 (dataset 2).

4 Figure 65a-5c shows the time-height variation of SNR,  $w$  and  $\sigma$  on 22 July 2011,  
5 depicting the typical diurnal evolution of ABL during the campaign period. The  $\theta_v$  profiles  
6 during morning-evening (at 08:24, 11:54, 14:25 and 17:15 IST) period are shown in Fig. 65d to  
7 depict the height of ABL (and also the gradients in  $\theta_v$  at the top of the ABL). Clearly, the height  
8 of ABL as obtained by the profiler (shown with dots on SNR plot) and radiosonde (the gradient  
9 in  $\theta_v$  profile) corresponds well. The agreement between them is also good in the diurnal  
10 variation, with both the measurements showing shallow ABL in the morning and evening  
11 transition periods and deep ABL during the day, when the ABL is convectively active.

12 The start time of AETAT as seen by different state variables at the surface and aloft on  
13 all days during the two campaigns is shown in Fig. 76a and 6b. It clearly reiterates the height  
14 dependency of start time of AETAT seen in Figs. 2-45, i.e., the start time of AETAT observed by  
15 profiler precedes surface state variables on all days and in both seasons. Though the same  
16 pattern is seen on all days, but the time at which the transition starts varies considerably from day  
17 to day.

18 The entrainment flux at the top of ABL is estimated by combining the measurements of  
19 radiosonde ( $\Delta\theta$ ,  $d_I$ ), profiler ( $w$ ,  $\Delta u_h$ ), MBLM ( $u$ ,  $\theta_{vo}$ ) and a meteorological flux tower ( $u_*$ ) with  
20 ECMWF interim data (advection term). The sensible heat flux and  $u_*$  at the surface required to  
21 quantify the entrainment ratio (Eq. 1) are estimated following the eddy covariance method by  
22 using 20 Hz resolution ultrasonic anemometer measurements at 8 m level. ~~A stringent data~~

1 ~~quality check has been performed for the estimation of fluxes (Burba, 2013).~~ These fluxes are  
2 evaluated at 30 min resolution.

3        Figures ~~86ea~~ and ~~6db~~ shows the sensible and entrainment fluxes at ~3 h resolution during  
4 the day, depicting the forcing on the ABL from bottom and top. The sensible heat flux varies  
5 considerably during the day, with fluxes varying from 0.15-0.25~~1.5-2.5~~ K ms<sup>-1</sup> around noon  
6 (~11:00 and ~14:00 IST) to 0.02-0.07 K ms<sup>-1</sup> during the morning and evening transitions (~08:00  
7 and ~17:00 IST). On the other hand, the entrainment flux neither changes drastically during the  
8 day nor shows a clear diurnal cycle (compared to sensible heat flux). The magnitude of  
9 entrainment flux depends mostly on the first term in Eq. 2, while the shear (2 and 3 terms in Eq.  
10 2) contributes very little to the total entrainment flux (not shown). ~~In contrast to large eddy~~  
11 ~~simulations (LES) by Canut et al. (2012), who found an increase of the entrainment rate in the~~  
12 ~~late afternoon, the present observations do not show any such increase, rather the entrainment~~  
13 ~~flux remained rather constant throughout the day on all days.~~ Since the buoyancy flux changes  
14 considerably, the entrainment ratio varies significantly during the course of the day. The  
15 entrainment ratio increases to 0.5-1.1 during the morning and evening transitions. Therefore, it is  
16 very clear from these observations that the forcing from the top (i.e., entrainment flux) becomes  
17 very important, when the buoyancy flux is weak (i.e., during the transitions and night) and plays  
18 ~~a decisive role in altering the structure of ABL.~~ A few earlier studies also underscored the  
19 importance of buoyancy flux in altering the structure of ABL. The entrainment ~~It is known from~~  
20 ~~earlier studies by Lohou et al. (2010) that the entrainment~~ not only modifies the top of the ABL  
21 but also impacts the entire depth of the ABL (Lohou et al., 2010). Caughey and Kaimal (1977),  
22 have shown experimentally that the heat flux descends suddenly during the transition,  
23 approximately an hour before the sunset, and the reversal of heat flux (from positive to negative)

1 first occurs at higher altitudes and then propagates downwards to the surface, indicating the  
2 importance of entrainment heat flux in the top-to-bottom evolution of the transition. Also, with  
3 continuous waning of sensible heat flux during the AETAT, both the vertical extent and strength  
4 of thermals (can be seen in Figs. 1 and 56) decrease monotonously. At the same time, the  
5 surface forcing (heating) remains good enough to maintain the turbulence close to the surface  
6 and therefore ~~doesn't~~ does not show the signature of transition, but delays it at the surface  
7 (Angevine, 2008). ~~The reduction in the vertical extent and strength of thermals and an increase in~~  
8 ~~entrainment ratio appear to be primarily responsible for the observed top to bottom evolution of~~  
9 ~~the start time of AET.~~

## 10 **5. Conclusions:**

11 This study presents a comprehensive view on the AETAT in terms of understanding the  
12 variability of different state variables using a suite of in-situ and remote sensing measurements  
13 at Gadanki. The study aims to address the following issues related to the start time of AETAT  
14 with a unique and statistically robust data set (~3 years). Which parameter first shows the  
15 signature of transition at the surface and aloft? Which parameter better defines or identifies it?  
16 How does it varies with altitude and season? follow any seasonal cycle? How does it varies  
17 with altitude? Which physical mechanism explains the observed vertical variation of transition?

18 (i) Among the surface state variables, the signature of transition is first seen in  $\sigma_{WS}^2$  and  $T$  data,  
19 both of which start decreasing monotonically ~100 min prior to the time of sunset. The  $r$   
20 increase is the last signature of transition, while the reversal of ~~sensible heat flux (in terms of  $\Delta T$~~   
21 ~~variation from positive to negative)~~ falls in between these extremes. Aloft, both SNR and  $\sigma$   
22 identify the start of AETAT at the same time, 120-160 min prior to the time of sunset, depending  
23 on the height considered. The observed mean start time of AETAT (2 h prior to the sunset),

1 obtained from SNR and  $\sigma$  variations, matches well with that obtained by Mahrt (1981), who used  
2 horizontal wind reduction for identifying the transition.

3 (ii) At the surface, the start time of AETAT can be discerned more easily from variations of  $T$   
4 than from that of  $\sigma_{WS}^2$ ,  $r$  and  $\Delta T$ . While  $\sigma_{WS}^2$  and  $\Delta T$  variations show large modulations with time,  
5  $r$  variation is ambiguous at times. Also, the temperature reduction is more consistent with  
6 relatively narrow distribution and occurs always before the sunset. Aloft, SNR variation is  
7 robust in identifying the transition compared to ambiguous variations in horizontal wind velocity  
8 (decreases at lower altitudes and increases at higher altitudes).

9 (iii) The start time of AETAT as defined by different state variables show some seasonal  
10 variation, with delayed transitions during the northeast monsoon at the surface and aloft. Though  
11 there is some seasonal variation in the start time of AETAT relative to sunset time, the order in  
12 which the signature of AETAT is seen in different state variables (first in  $T$ , and  $\sigma_{WS}^2$  followed  
13 by  $\Delta T$  and  $r$ ) remained nearly the same in all seasons.

14 (iv) Interestingly, the start time of AETAT exhibits a clear height dependency, i.e., the signature  
15 of transition is seen first in profiler attributes (~160 min) followed by sodar attributes (~120 min)  
16 and finally in surface state variables (~100 min), suggesting that the transition follows a top-to-  
17 bottom evolution (Angevine, 2008). The fact that the first signatures of transition are seen at  
18 higher altitudes by profiler/sodars than at the surface suggests that the forces other than the  
19 buoyancy could also play an important role during the transition. With continuous waning of  
20 sensible heat flux (and surface forcing) during the AETAT, both the vertical extent and strength  
21 of thermals decrease steadily (as seen in Figs. 1 and 56), triggering the ~~collapse~~ descend of ABL  
22 or transition. However, the surface heating is good enough to maintain the state variables and  
23 delay the decrease of  $T$  and  $\sigma_{WS}^2$  (considered to be the signatures of transition). Further, the



1 impact of forcings from top and bottom on the ABL is studied by quantifying the sensible and  
2 entrainment fluxes, using a flux tower and profiler-radiosonde measurements, respectively.  
3 Though the sensible heat flux varied significantly during the day, the entrainment flux remained  
4 nearly the same throughout the day. The entrainment ratio increases considerably during the  
5 morning and evening transitional periods, primarily due to the weak sensible heat flux.  
6 Therefore, the entrainment flux appears to be playing a major role during the transition period  
7 (and in the night) during which the sensible heat flux continuously weakens. ~~he reduction in the~~  
8 ~~strength and vertical extent of thermals and an increase in entrainment ratio are thought be~~  
9 ~~responsible for the observed top to bottom evolution of the transition.~~

10  
11 *Acknowledgements:-* The authors would like to thank M. Venkat Ratnam for providing the GPS  
12 radiosonde used in the present study (experiments are conducted under the special campaign of  
13 Tropical Tropopause Dynamics (TTD) as a part of CAWSES-Phase II programme, India).

14  
15  
16  
17  
18  
19  
20  
21  
22  
23  
24  
25  
26  
27

1  
2 | **REFERENCES:References**  
3 Acevedo, O. C., and Fitzjarrald, D. R.: The early evening surface-layer transition: Temporal and  
4 spatial variability, *J. Atmos. Sci.*, 11, 2650–2667, 2001.  
5 Anandan, V. K., Shrivankumar, M., and Srinivasarao, I.: First results of experimental tests of  
6 newly developed NARL phased array Doppler sodar, *J. Atmos. Oceanic Technol.*, 25,  
7 1778-1784, 2008.  
8 Angevine, W. M.: Entrainment results including advection and case studies from the Flatland  
9 boundary layer experiments, *J. Geophys. Res.*, 104, 30947-30963, 1999.  
10 Angevine, W. M.: Transitional, entraining, cloudy, and coastal boundary layers, *Acta Geophys.*,  
11 56, 2–20, 2008.  
12 Beare, R. J., Edwards, J. M., and Lapworth, A. J.: Simulation of the observed evening transition  
13 and nocturnal boundary layers: ~~large~~Large-eddy modelling, *Q. J. R. Meteorol. Soc.*, 132,  
14 61–80, 2006.  
15 Bonin, T., Phillip, C., Brett, Z., and Fedorovich, E.: Observations of the ~~Early-early Evening~~  
16 ~~evening~~ Boundaryboundary-~~Layer~~layer ~~Transition~~transition ~~Using~~using a ~~Small~~small  
17 ~~Unmanned~~unmanned ~~Aerial~~aerial ~~System~~system. ~~Boundary~~.-Lay. Meteorol.,\_146,\_119–  
18 132, 2013.  
19 Bosveld, F. C., Baas, P., Steeneveld, G. J., Holtslag, A. A. M., Angevine, W. M., Bazile, E.,  
20 Bruijn, E. I. F. D., Deacu, D., Edwards, J. M., Michael, E. K., Larson, V. E., Pleim, J. E.,  
21 Raschendorfer, M., and Svensson, G.: The third GABLS intercomparison case for  
22 evaluation studies of boundary-layer models. Part B: Results and process understanding,  
23 ~~Boundary~~.-Lay. Meteorol.,\_152, 157-187, doi:10.1007/s10546-014-9919-1, 2014.

1 Brazel, A. J., Fernando, H. J. S., Hunt, J. C. R., Selvor, N., Hedquist, B. C., and Pardyjak, E.:  
2 Evening ~~Transition~~-~~transition~~ ~~Observations~~-~~observations~~ in Phoenix, Arizona, J. Appl.  
3 Meteorol., 44,99-112, 2005.

4 Burba, G.: Eddy covariance method for scientific, industrial, agricultural, and regulatory  
5 applications, LI-COR Biosciences, Nebraska, 331pp., 2013.

6 Busse, J., and Knupp, K.: Observed characteristics of the ~~Afternoon~~afternoon ~~Evening~~-~~evening~~  
7 ~~Boundary~~-~~boundary~~ layer ~~Transition~~-~~transition~~ based on ~~Sodar~~-~~sodar~~ and ~~Surface~~-~~surface~~  
8 data, J. Appl. Meteorol. Climatol., 51,571-582, 2012.

9 ~~Canut, G., Couvreux, F., Lothon, M., Pino, D., and Said, F.: Observations and Large Eddy~~  
10 ~~Simulations of Entrainment in the Sheared Sahelian Boundary Layer, Boundary. Lay.~~  
11 ~~Meteorol., 142, 79-101, doi:10.1007/s10546-011-9661-x, 2012.~~

12 Caughey, S., and Kaimal, J.: Vertical heat flux in the convective boundary layer, Q. J. Roy.  
13 Meteor. Soc., 103, 811-815, 1977.

14 Dee, D. P., Uppala, S. M., Simmons, A. J., Berrisford, P., Poli, P., Kobayashi, S., Andrea, U.,  
15 Balmaseda, M. A., Balsamo, G., Bauer, P., Bechtold, P., Beljaar, A. C., van de Berg, L.,  
16 Bidlot, J., Bormann, N., Delsol, C., Dragani, R., Fuentes, M., Geer, A.J., Haimberger, L.,  
17 Healy, S. B., Hersbach, H., Hólm, E.V., Isaksen, L., Kållberg, P., Höhler, M., Matricardi,  
18 M., McNally, A. P., Monge-Sanz, M., Morcrette, J.-J., Park, B.-K., Peubey, C., de  
19 Rosnay, P., Tavolato, C., Thépaut, J.-N., and Vitart, F.: The ERA-Interim reanalysis:  
20 configuration and performance of the data assimilation system, Q. J. Roy. Meteor. Soc.,  
21 137, 553-597, 2011.

1 Edwards, J. M., Beare, R. J., and Lapworth, A. J.: Simulation of the observed evening transition  
2 and nocturnal boundary layers: Single-column modelling, Q. J. Roy. Meteor. Soc., 132,  
3 61–80, 2006.

4 Fernando, H. J. S., Verhoef, B., Sabatino, S. Di., Leo, L. S., and Park, S.: The Phoenix evening  
5 transition flow experiment (TRANSFLEX), ~~Boundary-Layer Meteorol.~~, 147, 443-468,  
6 doi: 10.1007/s10546-012-9795-5, 2013.

7 Grant, A. L. M.: An observational study of the evening transition boundary-layer, Q. J. Roy.  
8 Meteor. Soc., 123, 657–677, 1997.

9 Grimsdell, A.W., and Angevine, W.M.: Observations of the afternoon transition of the  
10 convective boundary layer, J. Appl. Meteor., 41, 3–11, 2002.

11 Klein, P. M., Hu, X. M., and Xue, M.: Impacts of ~~Mixing-mixing Processes-processes~~ in  
12 ~~Nocturnal-nocturnal Atmospheric-atmospheric Boundary-boundary Layer-layer~~ on ~~Urban~~  
13 ~~urban Ozone-ozone Concentrations-concentrations~~, ~~Boundary-Layer Meteorol.~~, 150, 107-  
14 130, doi: 10.1007/s10546-013-9864-4, 2014.

15 Lohou, F., Said, F., Lothon, M., Durand, P., and Serça, D.: Impact of ~~Boundary-boundary-Layer~~  
16 ~~Processes-processes~~ on ~~Nearnear-Surface-surface Turbulence-turbulence Within-within~~  
17 the West Africa ~~Monsoonmonsoon~~, ~~Boundary-Layer Meteorol.~~, 136, 1-23, 2010.

18 Lothon, M., Lohou, F., Pino, D., Couvreux, F., Pardyjak, E. R., Reuder, J., Vilà-Guerau de  
19 Arellano, J., Durand, P., Hartogensis, O., Legain, D., Augustin, P., Gioli, B., Lenschow,  
20 D. H., Faloon, I., Yagüe, C., Alexander, D. C., Angevine, W. M., Bargain, E., Barrié, J.,  
21 Bazile, E., Bezombes, Y., Blay-Carreras, E., van de Boer, A., Boichard, J. L., Bourdon,  
22 A., Butet, A., Campistron, B., de Coster, O., Cuxart, J., Dabas, A., Darbieu, C., Deboudt,  
23 K., Delbarre, H., Derrien, S., Flament, P., Fourmentin, M., Garai, A., Gibert, F., Graf, A.,

1 Groebner, J., Guichard, F., Jiménez, M. A., Jonassen, M., van den Kroonenberg, A.,  
2 Magliulo, V., Martin, S., Martinez, D., Mastrorillo, L., Moene, A. F., Molinos, F.,  
3 Moulin, E., Pietersen, H. P., Pigué, B., Pique, E., Román-Cascón, C., Rufin-Soler, C.,  
4 Saïd, F., Sastre-Marugán, M., Seity, Y., Steeneveld, G. J., Toscano, P., Traullé, O.,  
5 Tzanos, D., Wacker, S., Wildmann, N., and Zaldei, A.: The BLLAST field experiment:  
6 Boundary-Layer Late Afternoon and Sunset Turbulence, *Atmos. Chem. Phys.*, 14,  
7 10931–10960, doi:10.5194/acp-14-10931-2014, 2014.

8 Mahrt, L.: The early evening boundary layer transition, *Q. J. Roy. Meteor. Soc.*, 107, 329-343,  
9 1981.

10 Nadaeau, D. F., Pardyjak, E. R., and Higgins, C. W.: A simple ~~Model~~-model for the ~~Afternoon~~  
11 ~~afternoon~~ and ~~Early~~-early ~~Decay~~-decay of ~~Convective~~-convective ~~Turbulence~~-turbulence  
12 over ~~Different~~-different ~~Land~~-land surfaces, *Boundary-Lay. Meteorol.*, 141, 301-324,  
13 2011.

14 Nieuwstadt, F. T. M., and Brost, R. A.: The decay of convective turbulence, *J. Atmos. Sci.*, 43,  
15 ~~No. 6~~, 532-546, 1986.

16 Pino, D., Jonker, H. J. J., Arellano, ~~and~~ J. V. G., ~~and~~ Dosio, A.: Role of shear and the inversion  
17 strength during sunset turbulence over land: characteristic length scales, *Boundary-Lay.*  
18 *Meteorol.*, 121, 537-556, doi:10.1007/s10546-006-9080-6, 2006.

19 Poulos, S. G., Blumen, W., Fritts, D. C., Lundquist, J. K., Sun, J., Burns, S. P., Nappo, C., Banta,  
20 R., Newsom, R., Cuxart, J., Terradellas, E., Balsley, B., and Jensen, M.: A  
21 comprehensive investigation of the stable nocturnal boundary layer, *B. Am. Meteorol.*  
22 *Soc.*, 83, 555–581, 2002.

1 Rao, T. N., Rao, D. N., and Mohan, K.: Classification of tropical precipitating systems and  
2 associated Z–R relationships, J. Geophys. Res., 116, 17699–17711, 2001.

3 Rao, T. N., Kirankumar, N.V.P., Radhakrishna, B., Rao, D. N., and Nakamura, K.: Classification  
4 of tropical precipitating systems using wind profiler spectral moments part I: algorithm  
5 description and validation, J. Atmos. Ocean. Tech., 25, 884–897,  
6 doi:10.1175/2007JTECHA1031.1, 2008.

7 Rao, T. N., ~~B.~~ Radhakrishna, ~~B., K.~~ Nakamura, ~~K.,~~ and ~~N.~~ Prabhakara Rao, ~~N.~~: Differences in  
8 raindrop size distribution from southwest monsoon to northeast monsoon at Gadanki, Q.  
9 J. Roy. ~~at~~ Meteorol. Soc., 135, 1630-1637, 2009.

10 Reddy, K. K., Kozu, T., Nakamura, K., Ohno, Y., Srinivasulu, P., Anandan, V. K., Jain, A. R.,  
11 Rao, P. B., Rao, R. R., Vishwanathan, G., Rao, D. N.: Lower atmospheric wind profiler at  
12 Gadanki, tropical India: Initial results, Meteorol. Z., 10, 457-466, 2001.

13 Sandeep, A., Rao, T. N., Ramkiran, C. N., and Rao, S. V. B.: Differences in atmospheric  
14 boundary-layer characteristics between wet and dry episodes of the Indian summer  
15 monsoon, Bound~~ary~~. -Lay. Meteorol., 153, 217-236, doi: 10.1007/s10546-014-9945-z,  
16 2014.

17 Sastre, M., Yague, C., Roman, C. C., Maqueda, G., Salamanca, F., and Viana, S.: Evening  
18 transitions of the atmospheric boundary layers: characterization case studies and WRF  
19 simulations, Adv. Sci. Res., 8, 39-44, 2012.

20 Sorbjan, Z.: A numerical study of daily transitions in the convective boundary layer, Bound~~ary~~. -  
21 Lay. Meteorol., 123, 365-383, doi: 10.1007/s10546-006-9147-4, 2007.

22 Srinivasulu, P., Yasodha, P., Kamaraj, P., Jayaraman, A., Reddy, S. N., and Satyanarayana, S.:  
23 Simplified ~~Active-active Array-array L-Band-band Radar-radar~~ for ~~Atmospheric~~

1 | ~~atmospheric Wind-wind Profiling~~profiling: ~~Initial-initial Results~~results, J. Atmos.  
2 | ~~Oceanie. Technol.~~, 28, 1436-1447, doi: 10.1175/JTECH-D-11-00011.1, 2011.  
3 | Srinivasulu, P., Yasodha, P., Kamaraj, P., Rao, T. N., Jayaraman, A., Reddy, S. N., and  
4 | Satyanarayana, S.: 1280-MHz active array radar wind profiler for lower atmosphere:  
5 | System description and data validation, - J. Atmos. ~~Oceanie. Technol.~~, 29, 1455-1470,  
6 | doi:10.1175/JTECH-D-12-00030.1, 2012.  
7 | Stull, R.B.: The ~~Energetics-energetics~~ of ~~Entrainment-entrainment~~ ~~Across-across~~ a ~~Density~~  
8 | ~~density~~ ~~Interface~~interface, J. Atmos. Sci., 33, 1260-1267, 1976.  
9 | Sun, J., and Wang, Y.: Effect of the Entrainment Flux Ratio on the Relationship between  
10 | Entrainment Rate and Convective Richardson Number, ~~Boundary~~ -Lay. Meteorol., 126,  
11 | 237-247, doi:10.1007/s10546-007-9231-4, 2008.  
12 | Van de Wiel, B. J. H., Moene, A. F., Steenveld, G. J., Baas, P., Bosveld, F. C., and Holtslag, A.  
13 | A. M.: A ~~Conceptual-conceptual~~ ~~View-view~~ on ~~Inertial-inertial~~ ~~Oscillations-oscillations~~  
14 | and ~~Nocturnal-nocturnal~~ ~~Low-low~~ ~~Level-level~~ ~~Jets~~jets, J. Atmos. Sci., 67, 2679-2689, doi:  
15 | 10.1175/2010JAS3289.1, 2010.

16

17

18

19

20

21

22

23

24  
25  
26  
27

**Table 1.** Instruments used in the integrated approach, their operating frequency, height coverage, vertical and temporal resolutions and duration of data.

Instrument	Frequency of operation	Measured parameters	Height coverage	Vertical resolution	Temporal resolution	Period used
SODAR	1.8 kHz	SNR, winds and $\sigma$	0.03 - 1.5 km	30 m	27 sec	2007-2010
LAWP	1.357 GHz	SNR, winds and $\sigma$	0.3 - 4.2 km	150 m	~11 min	1999-2000
WPR <sub>8x8</sub>	1.280 GHz	SNR, winds and $\sigma$	0.3 - 6.15 km	150 m	~10 min	2010
WPR <sub>16x16</sub>	1.280 GHz	SNR, winds and $\sigma$	0.75 - 5.025 km	75 m	~10 min	2010-2011
MBLM		$T$ , $r$ , pressure, WS, WD and short wave radiation	5 - 15 m	5 m	1 s	2009-2011
GPS Radiosonde		$T$ , RH, pressure	0 - 30 km	100 m	3 h	17-19 January 2011 21-24 July 2011
50 m Tower		Sonic temperature, vertical wind	8 m		0.05 s	17-19 January 2011 21-24 July 2011

28  
29  
30  
31



32  
33  
34

**Table 2.** Details of measured parameters and sensors (make, model number, resolution and accuracy) on MBLM.

Parameter	Make	Model No.	Resolution	Measurement height	Accuracy
Wind Speed and Wind Direction	RM Young	05103V	1 Hz	5, 10 and 15m	0.3 m s <sup>-1</sup> and 2°
Temperature and Relative Humidity	Rotronics	Hygroclip S3	1 Hz	5, 10 and 15m	0.3° C and 2%
Pressure	Komoline	KDS-021	1 Hz	1.2 m	1hPa
Short Wave Radiation	Kipp & Zonen	CMP 6	1 Hz	1.2 m	1 W m <sup>-2</sup>

45  
46  
47  
48  
49  
50  
51  
52  
53  
54  
55  
56  
57  
58  
59  
60

61 **Table 3.** Major specifications of SODAR, LAWP, WPR<sub>8x8</sub> and WPR<sub>16x16</sub>

Parameter	SODAR	LAWP	WPR <sub>16X16</sub>	WPR <sub>8X8</sub>
Operating frequency	1.8 kHz	1357.5 MHz	1280 MHz	1280 MHz
Peak power	100 W	1 kW	1.2 kW	0.8 kW
Antenna array	1 m x 1 m	3.8 m x 3.8 m	2.8 m x 2.8 m	1.4 m x 1.4 m
Pulse width	180 ms	1 $\mu$ s (uncoded)	4 $\mu$ s (coded)	1 $\mu$ s (uncoded)
Inter pulse period ( $\mu$ s)	9x10 <sup>6</sup>	40	55	55
No. of Coherent Integrations	1	70	64	32
No. of Incoherent Integrations	1	100	20	20
No. of FFT points	4096	128	1024	1024
Beam width (deg)	4	3	5	6.5
Range resolution (m)	30	150	75	150
Beam directions*	N16, Z, E16	E15, Z, N15	E15, W15, Z, N15, S15	E10N10, W10S10, Z, W10N10, E10S10

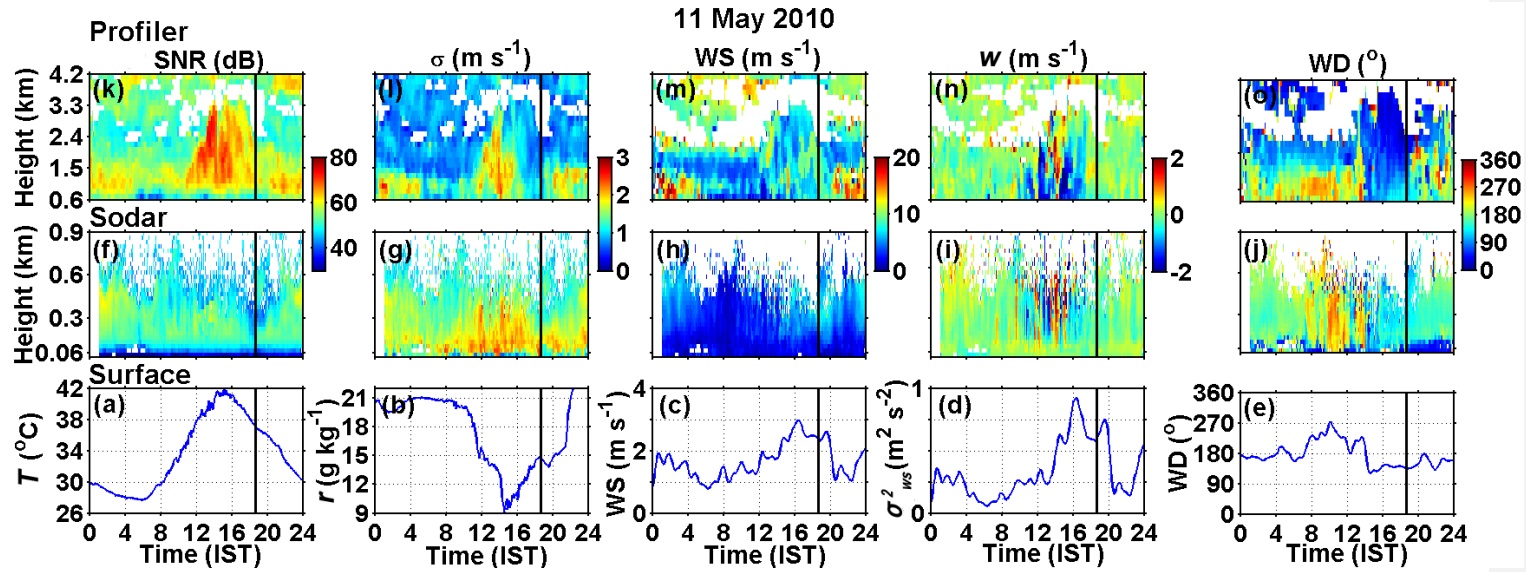
62 \* E, W, Z, N and S denote east, west, zenith, north and south directions, respectively, and the number indicates the off-zenith angle.

63  
64  
65  
66  
67  
68

1  
2 Table 4: Details of dataset 1 grouped as a function of season, showing the total number of days for which data are available, number of  
3 discarded days due to cloudy sky/rain or data gaps and number of clear days finally used in the present study. Win, Sum, SWM and  
4 NEM stand for, respectively, winter, summer, southwest monsoon and northeast monsoon.  
5

Season	15m Tower (2009-2011)				Sodar (2007-2010)				Profiler ( 1999-00, 2010-11)			
	Win	Sum	SWM	NEM	Win	Sum	SWM	NEM	Win	Sum	SWM	NEM
Total no. of days	113	195	263	221	207	333	414	255	108	238	381	264
Discarded days	25	55	158	130	105	152	282	189	41	101	227	140
Clear days	88	140	105	91	102	181	132	66	67	137	154	124

6  
7  
8  
9  
10

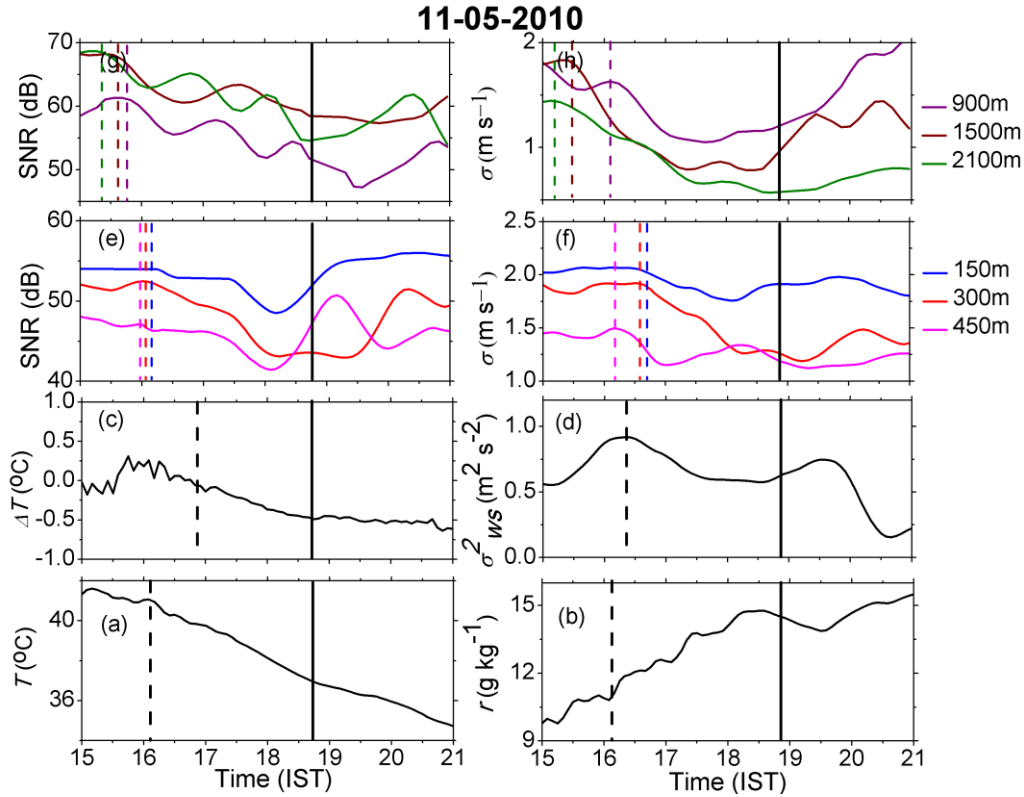


1

2 Figure 1: Diurnal variation of state variables at the surface and aloft on 11 May 2010, MBLM-derived surface (a)  $T$ , (b)  $r$ , (c)  $WS$  and  
 3 (d)  $\sigma_{ws}^2$  and (e)  $WD$  and sodar-derived (ef) range-corrected SNR, (fg)  $\sigma$ , (gh)  $WS$ , and (hi)  $w$  and (j)  $WD$ . (ik-lo) same as (ef-hj),  
 4 except for profiler-derived state variables. The solid vertical line indicates the time of sunset.

5

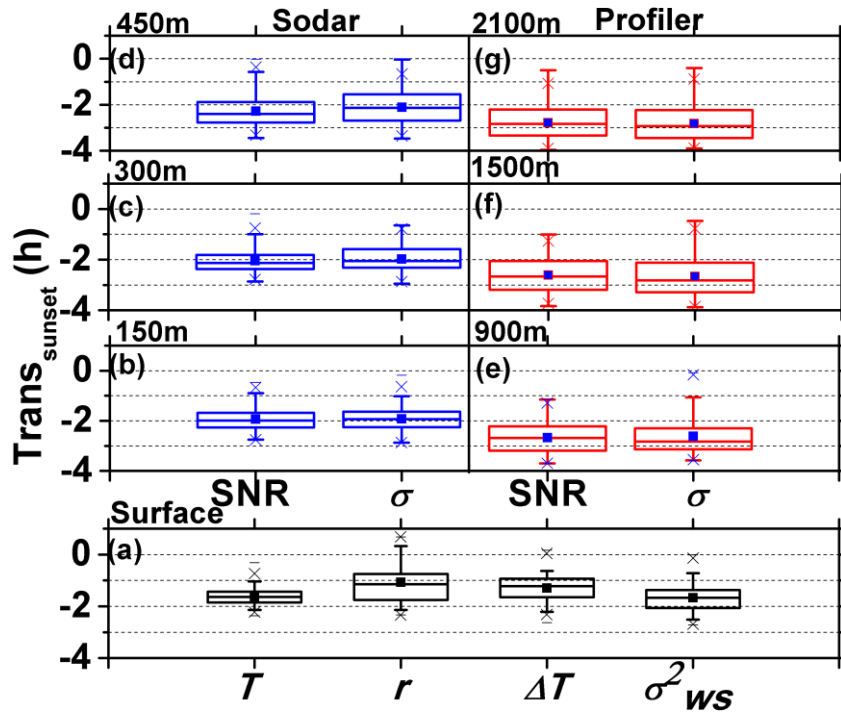
1



2  
3  
4  
5  
6  
7  
8  
9  
10  
11  
12  
13  
14  
15  
16  
17  
18

Figure 2: Temporal variation of state variables (at the surface and aloft) few hours before and after the time of sunset (indicated with a black solid vertical line). Temporal variation of MBLM-derived (a)  $T$ , (b)  $r$ , (c)  $\Delta T$  and (d)  $\sigma^2_{ws}$ , sodar-derived (e) range-corrected SNR and (f)  $\sigma$  and profiler-derived (g) range-corrected SNR and (h)  $\sigma$ . The sodar- and profiler-derived parameters are plotted at 3 representative levels each (150, 300 and 450 m for sodar and 900, 1500 and 2100 m for profiler, represented with different colours). Vertical dashed lines indicate the start time of the transition as identified by different state variables.

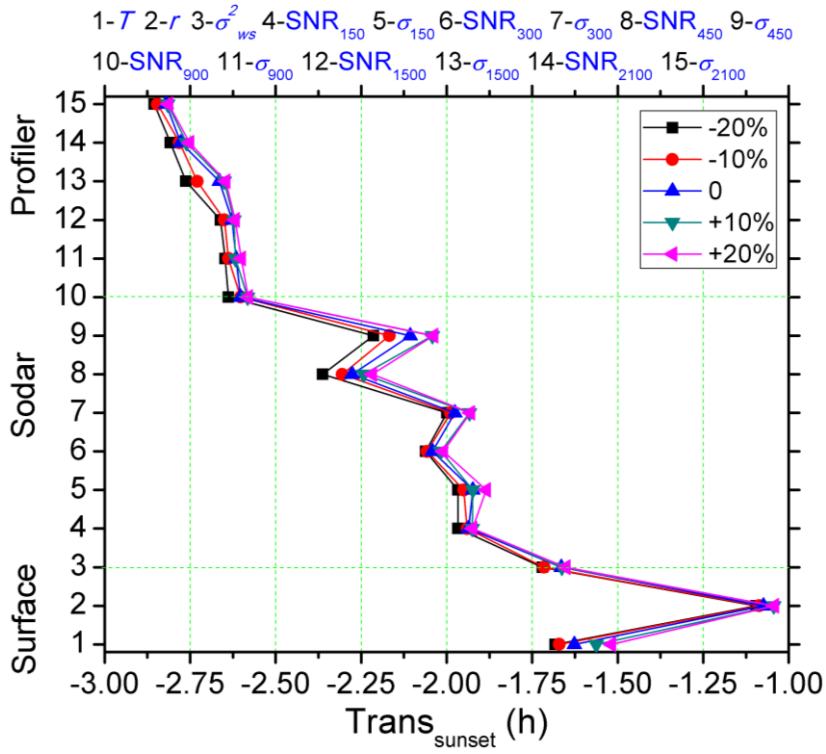
1  
2  
3



4  
5  
6  
7  
8  
9  
10  
11  
12  
13  
14  
15  
16  
17  
18  
19  
20  
21

Figure 3: Distributions (in terms of box plot) of  $\text{Trans}_{\text{sunset}}$  (= start time of  $\text{AETAT}$  - time of sunset) for different state variables, depicting the behaviour of transition start time with reference to the sunset time. Distributions for  $\text{Trans}_{\text{sunset}}$  at (a) the surface (obtained from  $T$ ,  $r$ ,  $\Delta T$  and  $\sigma^2_{ws}$ ), (b)-(d) 150 m, 300 m and 450 m, respectively (obtained from sodar-derived range-corrected SNR and  $\sigma$ ) and (e)-(g) 900 m, 1500 m and 2100 m, respectively (obtained from profiler-derived range-corrected SNR and  $\sigma$ ).

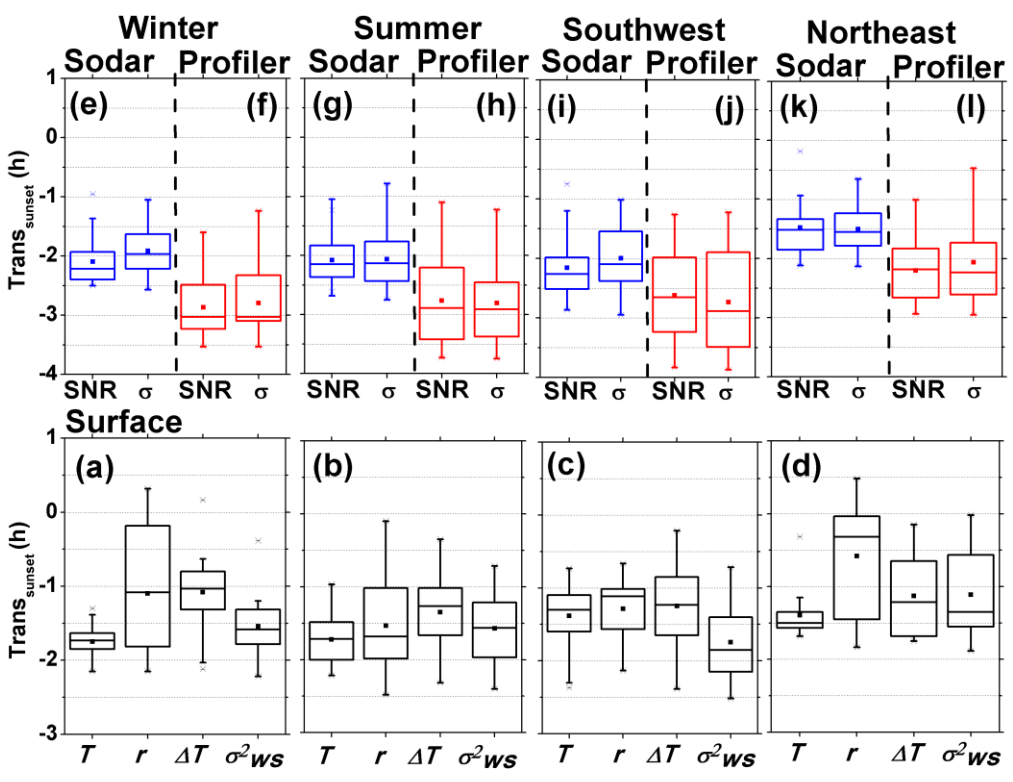
1  
2



3  
4  
5  
6  
7  
8  
9  
10  
11  
12  
13  
14  
15  
16  
17  
18  
19

Figure 4: Vertical variation of mean  $Trans_{\text{sunset}}$  as obtained by different state variables for different thresholds, depicting the sensitivity of thresholds used in the present study on the start time of transition.

1  
2

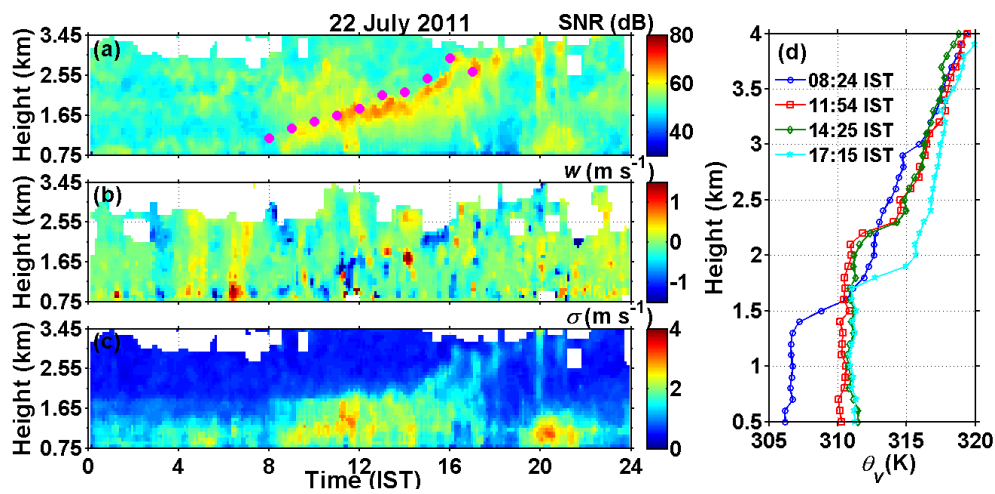


3  
4  
5  
6  
7  
8  
9  
10  
11  
12  
13  
14  
15  
16  
17  
18  
19

Figure 45: The distributions of  $Trans_{\text{sunset}}$  as obtained by different surface state variables for (a) winter (b) ~~summer~~premonsoon, (c) southwest monsoon and (d) northeast monsoon, depicting the seasonal variability in the start time of transition. The distributions for  $Trans_{\text{sunset}}$  as obtained by sodar-derived range-corrected SNR and  $\sigma$  at 300 m for (e) winter, (g) ~~premonsoon~~summer, (i) southwest monsoon and (k) northeast monsoon, respectively. (f), (h), (j) and (l) are same as (e), (g), (i) and (k), except for profiler-derived range-corrected SNR and  $\sigma$  at 1500 m.

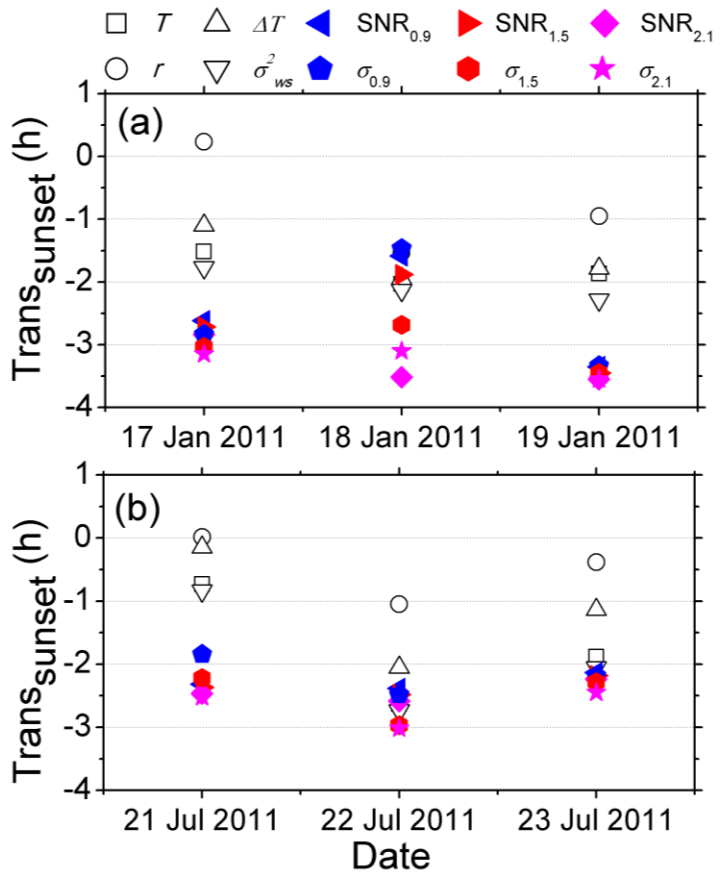


1  
2  
3  
4



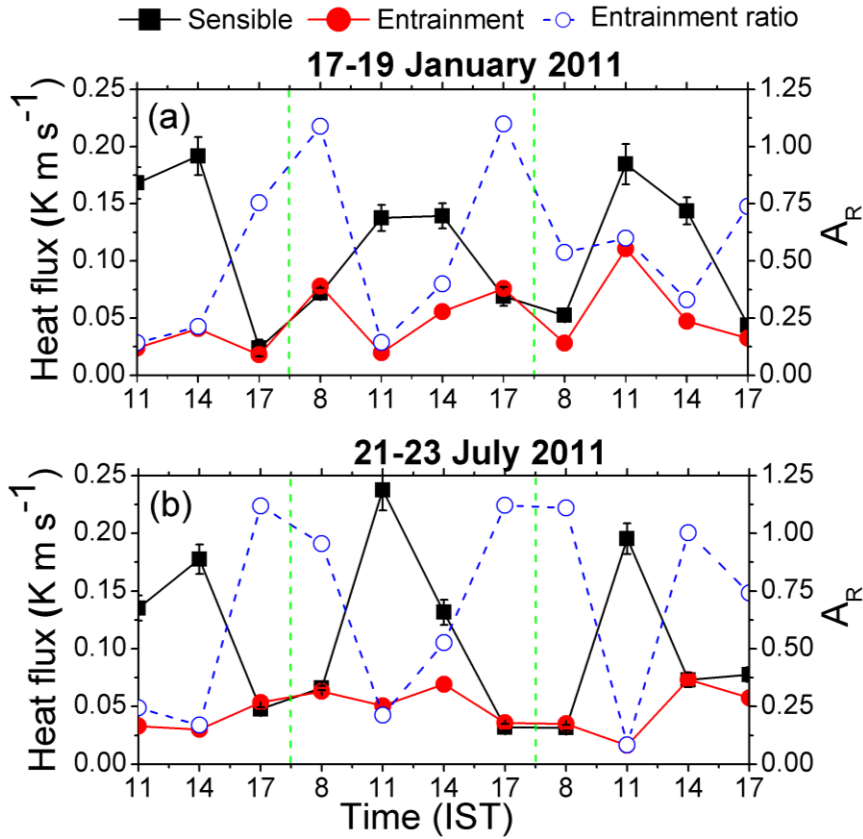
5  
6  
7  
8  
9  
10  
11  
12  
13  
14  
15  
16  
17  
18  
19  
20  
21  
22  
23  
24  
25  
26

Figure 56: Diurnal variation of ~~RADAR~~ profiler attributes (a) range-corrected SNR (b)  $w$  and (c)  $\sigma$  on 22 July 2011, illustrating the evolution of ABL and evening-afternoon transition. (d) The vertical variation of radiosonde-derived  $\theta_v$  at  $\sim 3$  h intervals. The solid symbols on (a) indicate the height of ABL.



1  
2  
3 | Figure 67: The start time of AETAT with reference to the time of sunset as obtained by different  
4 state variables at the surface and aloft during (a) 17-19 January 2011 and (b) 21 - 23 July 2011.  
5  
6  
7  
8  
9  
10  
11  
12  
13  
14  
15  
16

1  
2  
3



4  
5 Figure 8: (c) and (d) Sensible and entrainment fluxes (left axis) and entrainment ratios (right  
6 axis) estimated at ~3 h. intervals for during (a) 17-19 January 2011 and (b) 21-23 July 2011 the  
7 above days, indicating the forcings on ABL from the bottom and top.  
8

